

Aus der V. Medizinischen Klinik
der Medizinischen Fakultät Mannheim
(Direktor: Prof. Dr. med. Bernhard Karl Krämer)

Implications of the carnosine-carnosinase system in diabetic
nephropathy

Inauguraldissertation
zur Erlangung des medizinischen Doktorgrades
der
Medizinischen Fakultät Mannheim
der Ruprecht-Karls-Universität
zu
Heidelberg

vorgelegt von
Maria Angelica Rodriguez-Niño

aus
Bogota, Kolumbien

2019

Dekan: Prof. Dr. med. Sergij Goerd

Referent: Prof. Dr. rer.nat. B.A. Yard

Meine Familie
Fernando, Claudia und Daniela

TABLE OF CONTENTS

	Page
ABBREVIATIONS	1
1 INTRODUCTION	6
1.1 Diabetes mellitus: Definition and epidemiology	6
1.2 Diabetic nephropathy	7
1.2.1 Epidemiology	7
1.2.2 Pathophysiology and current therapies	7
1.3 Methylglyoxal: Role of carbonyl and oxidative stress	9
1.4 Assessment of the GSH redox potential by GFP coupled- redox sensors	9
1.5 The carnosine-carnosinase system	11
1.5.1 Carnosine	11
1.5.2 Carnosinase	13
1.6 Aim of the study	15
2 MATERIALS AND METHODS	17
2.1 Materials	17
2.1.1 Chemicals	17
2.1.1.1 Comercial chemicals	17
2.1.2 Antibodies	20
2.1.3 Restriction enzymes and buffer	20
2.2 Methods	24
2.2.1 Participant recruitment and sampling	24
2.2.2 ELISA assays	26
2.2.3 CN1 enzymatic activities	27
2.2.4 Generation of hCN1 transgenic mice	27
2.2.5 DNA isolation and sampling for animal experiments	27

2.2.6	CNDP1 genotyping.....	28
2.2.7	Protein precipitation and Westernblotting.....	28
2.2.8	HUVECs isolation.....	29
2.2.9	Cell Culture	29
2.2.10	Cell viability assay	30
2.2.11	DNA damage assay	30
2.2.12	Subcloning of roGFP and lentivirus production	30
2.2.13	Lentivirus transduction and titration.....	31
2.2.14	Radiometric measurements	32
2.2.15	Statistical analysis	33
3	RESULTS.....	34
3.1	Detection of Carnosinase1 in urine	34
3.2	Characterization of 24h urinary CN1 in living kidney donors and T2DM patients (DIALECT cohort).....	36
3.3	Association of serum CN1 and CNDP1 genotype with urinary CN1 in patients with T2DM and non-diabetic CKD.....	40
3.4	Toxicity profile of Methylglyoxal in human vascular endothelium	47
3.5	Carnosine treatment ameliorates MGO-induced toxicity	49
3.6	Characterization of a green fluorescent protein (roGFP) - based redox biosensor	52
4	DISCUSSION	57
4.1	Detection of Carnosinase1 in urine	57
4.2	Characterization of 24-hr urinary CN1 in living kidney donors and patients with T2DM (DIALECT cohort).....	57
4.3	Association of serum CN1 and CNDP1 genotype with urinary CN1 in patients with T2DM and non-diabetic chronic kidney disease (Mannheim Cohort).....	59
4.4	Toxicity profile of Methylglyoxal in human vascular endothelium	62
4.5	Carnosine treatment ameliorates MGO-induced toxicity	63
4.6	Characterization of a green fluorescent protein (roGFP)-based redox biosensor	64

5 CONCLUSION	66
6 REFERENCES	67
7 CURRICULUM VITAE.....	76
8 ACKNOWLEDGMENTS.....	77

ABBREVIATIONS

°C	grad Celsius
μ	micro (10 ⁻⁶)
5L/5L	homozygous for 5-leucin-repeats at micro-satellite marker D18S880 of CN1
Ab	Antibody
ACE	Angiotensin Converting Enzyme
ACEi	Angiotensin converting enzyme inhibitor
ACR	albumin creatinine ratio
ADA	American Diabetes Association
AER	Albumin excretion rate
AGEs	advanced glycation end products
ALEs	advanced lipoxidation end products
APS	ammoniumpersulfate
ARB	angiotensin converting enzyme blocker
ATLAS	anti- <i>CNDP1</i> antibody produced in rabbit from Sigma-Aldrich
ATP	adenosine triphosphate
BMI	body mass index
bp	base pair
BSA	bovine serum albumin
BTBR	Black and Tan, BRachyuric
BUN	blood urea nitrogen
cAMP	cyclic adenosine monophosphate
CARNS	carnosine synthase
cDNA	complementary DNA
CKD	chronic kidney disease
Cl	chloride
CN1	carnosinase
CNDP1	carnosinase dipeptidase 1 gene
COX-1	cyclo-oxygenase 1
Cr	creatinine
CTG	cytosine-thymine-guanine
dATP	deoxy-adenosine triphosphate
db	diabetes

DBP	diastolic blood pressure
dCTP	deoxy-cytidinetriphosphate
ddH ₂ O	double-distilled water
dGTP	deoxy-guanosinetriphosphate
DKD	diabetic kidney disease
DM	diabetes mellitus
DMSO	dimethylsulfoxide
DN	diabetic nephropathy
DNA	deoxyribonucleic acid
dNTP	dideoxy-nucleoside triphosphate
DTT	dithiothreitol
E. coli	Escherichia coli
EDTA	ethylene diaminetetraacetic acid
eGFR	estimated glomerular filtration rate
ELISA	enzyme-linked immunosorbent assay
ESRD	end stage renal disease
F	forward or phenylalanine
Fig.	figure
FPG	fasting plasma glucose
g	gram
G	glycine or guanine
Glo-1	Glyoxalase-1
Glo-2	Glyoxalase-2
GBM	glomerular basement membrane
GFP	green fluorescent protein
GFR	glomerular filtration rate
GLP-1	Glucagon-like peptide-1
GPX	glutathione peroxidase
GRX	glutaredoxin
GSH	glutathione
GSSG	glutathione disulfide
H ₂ O ₂	hydrogen peroxide
HbA1c	glycated hemoglobin
HCD	histidine-containing peptide
HCl	hydrogen chloride

hCN1	human CN1
HNE	4-Hydroxy-2-nonenal
hr(s)	hour(s)
HUVECs	human umbilical vein endothelial cells
HRP	horseradish peroxidase
IDNT	Irbesartan Diabetic Nephropathy Trial
IgG	immunoglobulin G
IU	international units
JNK	c-Jun N-terminal kinases
K	potassium
kb	kilo base pair
KCl	potassium chloride
kDa	kilo-dalton
KDIGO	Kidney Disease Improving Global Outcomes
kg	kilogram
l	liter
L	leucin
Log	logarithm
m	milli
M	molar (mol/l)
MAPK	mitogen-activated protein kinase
MGO	Methylglyoxal
Mg	Magnesium
MgCl ₂	magnesium chloride
min	minute
mRNA	messenger RNA
n	nano (10 ⁻⁹)
Na	sodium
NF	nuclease free
NF-κB	nuclear factor kappa-light-chain-enhancer of activated B cells
ns	not significant
nm	nanometer
nt	nucleotide
OD	optical density
ob	obesity

OGTT	oral glucose tolerance test
PBS	phosphate buffered saline
PCR	polymerase chain reaction
POD	peroxidase
PVDF	polyvinylidene fluoride
R	reverse
RAS	renin angiotensin system
Redox	reduction–oxidation reaction
RENAAL	Reduction in End-Points in Non-Insulin Dependent Diabetes Mellitus With the Angiotensin II Antagonist Losartan
RNA	ribonucleic acid
RNAse	ribonuclease
RCS	reactive carbonyl species
ROS	reactive oxygen species
rpm	revolutions per minute
RT	room temperature
RT-PCR	reverse transcription polymerase chain reaction
s	second
sAlb	serum albumin
SBP	systolic blood pressure
Scr	serum creatinine
SD	standard deviation
SDS	sodium dodecyl sulfate
SDS-PAGE	SDS-Polyacrylamide-Gel-electrophoresis
seq	sequence
SGLT	Sodium-glucose linked transporter
SOD	superoxide dismutase
STZ	streptozotocin
T1DM	type 1 diabetes
T2DM	type 2 diabetes
TAE	Tris-Acetate-EDTA
Taq	thermostable DNA-polymerase
TBS	Tris buffered saline
TBS-T	Tris buffered saline with 0,01% Tween20
TEMED	Tetramethylethylenediamine

TG	Triglyceride
Tris	Tris(hydroxymethyl)-aminoethane
Tm	melting temperature
TTR	transthyretin
UACR	urine albumin creatinine ratio
uAlb	urine albumin
uCr	urine creatinine
UMM	Clinical Faculty Mannheim (Universitätsklinikum Mannheim)
UV	ultraviolet
USA	United States of America
UF	ultrafiltration
W	watt
wt	wild type
Zn	zinc

1 INTRODUCTION

1.1 Diabetes mellitus: Definition and epidemiology

Diabetes Mellitus is a metabolic disorder characterized by chronic hyperglycemia affecting more than 425 million worldwide¹. It imparts high morbidity and mortality and thus it is considered a major health problem urging to take action to reduce health care costs². There are two main types of diabetes Mellitus, i.e. type 1 and type 2, of which the latter contributes foremost to the overall prevalence². Type 1 diabetes mellitus (T1DM) is an auto-immune disease in which destruction of beta cells leads to absolute insulin deficiency and consequently to hyperglycemia. In contrast, T2DM is initially driven by insulin resistance followed by a progressive decrease in insulin secretory capacity with time. Apart from age and lifestyle-related factors also genetic factors contribute to the development of T2DM. As such T2DM aggregates in families with currently more than 60 genetic traits reported to be associated with risks to develop diabetes³.

Diabetes is not only associated with microvascular complications (nephropathy, neuropathy and retinopathy) but also accelerates atherosclerosis independently of other traditional cardiovascular risk factors^{4,5}. Although the risk for developing microvascular complications is proportional to both the severity and duration of hyperglycemia⁶, T2DM is usually not detected until late in the course of cardiovascular disease (CVD) and therefore, many patients are already suffering from complications at or shortly after diagnosis of T2DM. Because of the strong association between diabetes and cardiovascular disease (CVD)⁷, cardiovascular mortality in diabetic patients is high, accounting for 52% of deaths in T2DM and 44% in type 1 diabetes mellitus (T1DM)⁸.

According to the American Diabetes Association (ADA), diabetes is diagnosed based on plasma glucose parameters, i.e. fasting plasma glucose (FPG), oral glucose tolerance test (OGTT)⁹, or the recently added HbA1c criteria¹⁰. HbA1c is an indicator of chronic glycaemia reflecting average glucose levels over a period of 2-3 months and it is used as a standard biomarker of proper glycemic management¹¹.

Although the currently used therapeutics targets, e.g. blood pressure-¹², lipid¹³⁻¹⁵ and glycemic control¹⁶⁻¹⁸, have proven to be highly efficacious to decrease the

incidence and to retard the progression of microvascular complications, the association of tight glycemic control and reduction of macrovascular complications is more ambiguous¹⁹. Recent clinical interventions trials with new therapeutics such as sodium glucose cotransport (SGLT-2) inhibitors and glucagon-like peptide (GLP-1) agonists have consistently demonstrated cardiovascular benefits and weight loss effects in patients with T2DM^{20–23}. Yet, early screening and early lifestyle intervention programs are likely to be the most efficacious and cost reducing strategies to counteract the increasing incidence of T2DM and its associated complications²⁴.

1.2 Diabetic nephropathy

1.2.1 Epidemiology

Diabetic nephropathy (DN) is considered to be one of the most devastating microvascular complications of diabetes mellitus, developing in nearly one third of patients with type 1 or type 2 diabetes²⁵. It is by far the most common cause of chronic kidney disease (CKD) worldwide, frequently leading to end-stage renal disease (ESRD) and the need for renal replacement therapy²⁶. The prevalence of DN largely differs amongst ethnic groups, with Native Americans, African Americans and indigenous Australians having the highest prevalence of ESRD due to diabetes²⁷.

DN also imparts an increased risk for cardiovascular disease and death in patients with type 1 and type 2 diabetes²⁸. Accordingly, the annual cardiovascular death rate is 2% and 3.5% in patients with microalbuminuria and macroalbuminuria respectively, increasing up to 12.1% in patients on renal replacement therapy²⁹.

1.2.2 Pathophysiology and current therapies

DN typically develops through sequential phases, commonly starting with a supraphysiologic increase in the glomerular filtration rate (GFR) known as hyperfiltration. This phenomenon is an adaptive response to functional nephron mass reduction and to hemodynamic and metabolic changes prevailing in diabetes and obesity³⁰.

This increase in GFR is followed by intermittent episodes of microalbuminuria which progress to persistent microalbuminuria in one third of the patients and reflects an

initial loss of permselectivity of the glomerular basement membrane. Thus, abnormalities in albuminuria excretion are often the first clinical manifestation of DN. The classification of albuminuria according to the Kidney Disease Improving Global Outcomes (KDIGO) guidelines 2012 are displayed in Table 1.³¹.

Table 1. Albuminuria categories according to KDIGO 2012

Category	AER ^b (mg/24h)	ACR ^a (approximate equivalent)		Terms
		(mg/mmol)	(mg/g)	
A1	<30	<3	<30	Normal to mildly increased
A2	30-300	3-30	30-300	Moderately increased
A3	>300	>30	>300	Severely increased

^aAlbumin-to-creatinine ratio, ^b Albumin excretion rate

The stage of microalbuminuria is followed by macroalbuminuria and progressive decline in GFR^{32,33}. These clinical signs are often associated with structural pathological changes such as podocyte injury, mesangial expansion and glomerulosclerosis³⁴.

The increase in albuminuria is often accompanied by comorbidities such as diabetic retinopathy and hypertension. In the last stage of the disease, decline in GFR progresses to ESRD which ultimately results in the need of renal replacement therapy. Importantly, both low GFR and albuminuria are independent predictors of mortality and progression to ESRD³⁵.

Current treatment modalities for diabetic nephropathy focus on four main targets: cardiovascular risk reduction, glycemic control, blood pressure control and inhibition of the renin-angiotensin system (RAS)³⁶. Observational data from large clinical intervention trials in patients with T2DM and proteinuria, i.e. IDNT (Irbesartan Diabetic Nephropathy Trial) and the RENAAL (Reduction in End-Points in Non-Insulin Dependent Diabetes Mellitus With the Angiotensin II Antagonist Losartan) have demonstrated that RAS blockade with angiotensin converting enzyme (ACE) inhibitors or angiotensin receptor blockers (ARBs) retards disease onset and progression of albuminuria, independently of blood pressure control³⁷⁻³⁹. Additionally, emerging therapies such as the SGLT2 inhibitors have been recently approved for the treatment of diabetes and have shown positive effects on renal outcomes³⁶.

1.3 Methylglyoxal: Role of carbonyl and oxidative stress

Although the value of appropriate glycemic control in diabetic patients is indisputable, some T2DM patients with HbA1c below the diabetes definition threshold still develop microvascular complications⁴⁰. This raises the question as to whether additional mechanisms might be involved in onset and disease progression of such complications⁴¹. Compelling evidence has suggested a role for methylglyoxal (MGO) as pivotal mediator of diabetic complications. In line with this, elevated levels of MGO in serum and tissues of patients with diabetes and ESRD have been reported^{42,43}. MGO is a reactive metabolite and a byproduct of carbohydrate, lipid and amino acid metabolisms. MGO reacts with proteins and nucleic acids causing protein malfunction and formation of advanced glycation end-products (AGEs)⁴⁴.

Exogenous administration of MGO in animals or in *in vitro* systems results in pathological changes seen in diabetic conditions such as microvascular damage and insulin resistance⁴⁵⁻⁴⁷. Compatible with this, is the remarkable finding that elevated levels of endogenous MGO in glyoxalase-1 (Glo-1) knockout drosophila is sufficient to recapitulate the phenotype of T2DM, namely obesity, insulin resistance and hyperglycemia⁴¹. Similarly, knockdown of Glo-1 in a non-diabetic mice model, results in renal lesions similar to the ones found in diabetic mice models⁴⁸.

MGO might also elicit an inflammatory response through the formation of reactive oxygen species (ROS). Pathological concentrations of MGO provoke a rapid production of ROS in human aortic endothelial cells⁴⁹. In human vascular endothelium, MGO-induced inflammation is mediated via the activation COX-2, JNK and p38 MAP kinase⁵⁰. At transcriptional level, MGO treatment elicits a strong upregulation of cell cycle arrest-associated genes, compatible with a possible activation of the p53 pathway⁵¹.

During detoxification through the glyoxalase system, MGO reacts with reduced glutathione (GSH) and it is converted to S-D-lactoylglutathione⁵². The latter is further metabolized to lactate and GSH through the action of Glo-2.

1.4 Assessment of the GSH redox potential by GFP coupled- redox sensors

Under physiological conditions cells produce low amounts of ROS which are, amongst others, involved in modulating cell growth, differentiation, metabolism and

immune responses. Alterations in the cellular reduction-oxidation (redox) equilibrium are reflected by changes of the redox couples, i.e. reduced/oxidized thioredoxin and glutathione/glutathione disulfide (GSH/GSSG)⁵³. The latter is considered to have a major role in maintaining intracellular redox equilibrium and is the most important redox buffer in almost all eukaryotic cells⁵⁴.

Measurement and quantification of the cellular redox status with conventional tools often lack specificity for the redox pair in question and usually require cell lysis which introduce oxidation artefacts in the system⁵⁵. In recent years, genetically encoded fluorescent sensors appeared to overcome these limitations allowing real-time assessment of the intracellular redox status. These probes make use of the green fluorescent protein (GFP) which has been widely used in biology for molecular labeling and protein tagging since its discovery in 1962⁵⁶. Wild type GFP has a single emission peak at 509 nm⁵⁵, while it has two excitation peaks with a maximum at 395 nm and 475 nm respectively. These correspond to the protonated-neutral and the deprotonated-anionic form of the chromophore. The dual excitation behavior can be exploited for radiometric measurements. One of the many advantages of the radiometric indicators is that it minimizes measurement errors resulting from changes in indicator concentrations, photobleaching, illumination stability and imaging artefacts^{54,55}.

Different indicators of the redox status such as roGFP1 and roGFP2 have been constructed by substitution of specific surface-exposed residues with cysteines in the β -barrel structure in close proximity to the chromophore of GFP^{53,54}. Disulfide bonds between these cysteine residues promotes protonation of the chromophore and increases the excitation spectrum resulting in enhancement of GFP fluorescent properties⁵³.

RoGFP sensors report dynamic redox changes in response to a variety of exogenous membrane-permeable oxidizing and reducing agents. Typically, these responses have been described for incubation with H₂O₂ and dithiothreitol (DTT), however it is not sufficiently clear which endogenous redox pair interact with roGFP^{53,54}. Furthermore, the use of roGFP sensors is also limited by their slow response to changes in the redox potential⁵⁷. Based on these limitations, Gutscher et. al rationalized to equip the sensor with Glutaredoxin1 (Grx1)(Grx1-roGFP) which

specifically catalyzes the equilibrium between the two redox pairs $\text{roGFP2}_{\text{reduced}}/\text{roGFP2}_{\text{oxidized}}$ and GSH/GSSG (**Fig.1**)⁵⁷.

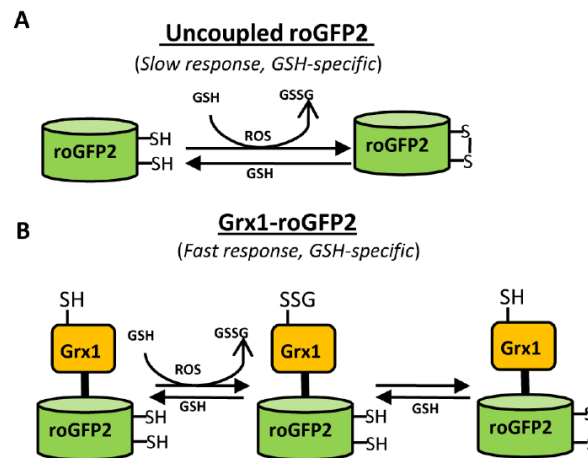


Fig.1 RoGFP-Based sensors. (A) roGFP contains cystein residues capable of forming a disulfide bond in response to changes in intracellular glutathione redox potential. The redox equilibrium of roGFP with the GSH/GSSG couple occurs through endogenous glutaredoxins and proceeds slowly. (B) The fusion of Grx1 to roGFP substantially improves specificity and reaction rate of thiol-disulfide exchange between roGFP dithiol and 2GSH/ GSSG couple. Adapted from Bhaskar et. al⁵⁸.

Upon an oxidative stressor, a cysteine residue of Grx1 specifically reacts with GSSG to form a Grx1-gluthatione disulfide intermediate which will react with one of the two thiols on roGFP. This reaction results in S-gluthationylation. In the last step, gluthationylated roGFP re-arranges forming an internal disulfide bridge. When the oxidative event is removed, GSSG rapidly normalize resulting in the equilibrium of the thiol/disulfide cascade⁵⁵ (**Fig.1**). Thus, the response of Grx1-roGFP is a dynamic probe which rapidly equilibrates with intracellular GSH/GSSG couple. This improved version of the sensor also allows the detection of short and long lived reflections of GSH. Consequently, the oxidation of Grx1-roGFP by GSSG is 100.000 times faster compared to uncoupled roGFP.

1.5 The carnosine-carnosinase system

1.5.1 Carnosine

Carnosine is a natural occurring dipeptide, composed of β -alanine and L-histidine, and synthesized by the carnosine synthase (CARNS) enzyme⁵⁹. In mammalian tissues, carnosine is widely distributed but predominantly found in the olfactory bulb

of the brain and in skeletal muscle. In the latter, carnosine can be found in relatively high concentrations (10- 40 mmol/ kg of dry tissue)⁶⁰.

Endowed by a plethora of biological properties carnosine has been subject in a wide range of scientific fields, particularly in the context of muscle physiology, metabolic disorders and oxidative stress conditions.

Carnosine acts as a physiological buffer and this property is mostly attributed to its characteristic imidazole ring and its pK_a (6.72) which is close to the physiological pH⁶¹. In muscle, carnosine plays an important role in the contractile function of skeletal fibers and calcium handling⁶¹. Furthermore, human studies have shown that the degree of blood acidosis during high-intensity exercise is alleviated, when muscle carnosine content is increased⁶². Thus, high carnosine concentrations in muscle appear to improve high intensity exercise performance⁶².

The beneficial effect of carnosine in metabolic diseases, e.g. diabetes and hyperlipidemia, is widely reported. In streptozotocin-induced diabetic rats carnosine supplementation reduced hyperglycemia and hyperlipidemia⁶³. Similarly, glucose lowering effects and preservation of pancreatic β -cell mass were reported in carnosine-fed db/db diabetic mice⁶⁴. In BTBR^{ob/ob} mice, which develop advanced features of diabetic nephropathy, carnosine treatment attenuated albuminuria, reduced mesangial matrix expansion and improved other glomerular anomalies of diabetic nephropathy⁶⁵. Furthermore, inhibition of pro-apoptotic signaling and podocyte loss were prevented by carnosine feeding in streptozotocin-diabetic induced rats⁶⁶. Interestingly, in db/db mice carnosine appeared to accelerate wound healing and increased expression of growth factors and cytokine genes involved in reparative processes⁶⁷.

Numerous mechanisms may underlie the beneficial effect of carnosine to improve metabolic condition. Discussed are carnosine's antioxidant properties, its ability to reverse protein glycation, and its ability to reduce AGE and advanced lipoxidation end-product (ALE) formation. Carnosine's antioxidant activity involves scavenging of reactive oxygen species (ROS) such as hydroxyl- and superoxide radicals, but also involves the upregulation of antioxidant enzymes⁶¹. Accordingly, carnosine treatment was found to reduce markers of lipid oxidation and to restore the depleted levels of glutathione (GSH) and the basal activities of SOD and glutathione peroxidase (GPX) in the liver and heart of aged rats⁶⁸.

The anti-glycating properties of carnosine have been repeatedly reported *in vitro* and *in vivo*. Compelling evidence suggests that carnosine acts at different stages of AGEs formation, i.e. from reversing the formation of Schiff bases (first product of protein glycation) to reversal of preexisting glycated proteins⁶⁹⁻⁷¹. Furthermore, carnosine reacts strongly with 4-hydroxy-trans-2,3-nonenal (4-HNE), the most abundant class of ALE precursors, and forms stable carnosine-HNE reaction adducts^{65,72,73}. Since the production and accumulation of ALEs and AGEs are important mediators in diabetic complications, the use of carnosine has gained prominent scientific interest and numerous *in vivo* and *in vitro* diabetes relevant studies have reported positive results to diminish or prevent diabetic associated complications. Furthermore, recent data from a clinical trial confirmed to some extent carnosine beneficial effects in pre-diabetic obese patients^{74,75}.

1.5.2 Carnosinase

Carnosinase (CN1), encoded by the CNDP1 gene, was first described by Teufel et. al as a dipeptidase belonging to the metalloproteases family. CN1 is the rate-limiting enzyme for the hydrolysis of carnosine into alanine and histidine, and also other histidine-containing peptides, i.e. anserine and homocarnosine⁷⁶.

One of the first reports suggesting a link between DN and CN1 came from the finding that a trinucleotide repeat ((CTG)_n) polymorphism in the CNDP1 gene was associated with susceptibility to develop DN. The finding showed that patients with T2DM and homozygous for the short allelic variant (CTG)₅, also referred as the *Mannheim allele*, have a lower risk of developing DN.⁷⁷

Thereafter, multiple studies have consistently confirmed the association between this polymorphism and susceptibility to develop DN in T2DM of different ethnicities^{78,79}. Interestingly, this association has been suggested to be sex-specific⁸⁰.

Nonetheless, it should also be mentioned that studies in patients of african-american and mexican-american ethnicity have failed to demonstrate this association.^{81,82}

In patients with type 1 diabetes there are also inconsistent findings related to the association between CNDP1 and ESRD. While in a genome-wide SNP genotyping approach in unrelated Caucasian individuals with type 1 diabetes an association between ESRD and CNDP1 was observed⁸³, this was not found in another case-control study of caucasian patients with type 1 diabetes⁸⁴. Likewise, Alkhalaf et al. did

not find an association between the homozygous CNDP1(CTG)₅ genotype and DN in patients with type 1 diabetes, but rather an increased risk for progression to ESRD late after baseline measurements⁸⁵.

The influence of the CNDP1 Mannheim allele has also been investigated in non-diabetic nephropathies. Accordingly, studies have showed that the (CTG)₅ is associated with a slower progression to CKD and to slightly correlate with renal survival in patients with glomerulopathies but not in patients with tubulointerstitial disease^{86,87}.

The (CTG)_n polymorphism located within the signal sequence of the CNDP1 gene is functional as it influences the efficacy of CN1 secretion from the liver into the circulation⁸⁸. The shortest allelic form (CTG)₅, has been associated with low CN1 enzymatic activities and serum concentrations which presumably allows higher tissue carnosine concentrations affording protection against hyperglycemia-mediated tissue damage^{77,88} (**Fig.2**).

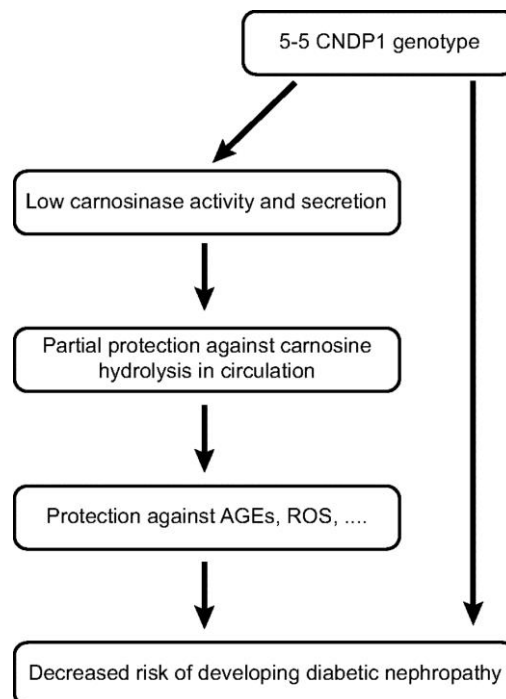


Fig.2 Proposed link between the (CTG)₅ in the CNDP1 gene and susceptibility to develop diabetic nephropathy, adapted from Boldyrev et. al⁶¹.

Apart from hyperglycemia and the (CTG)_n polymorphism, a recent study suggest that renal function might also influence CN1 concentrations in serum of patients with T2DM⁸⁹.

In rodents, CN1 is not a secreted protein and its expression is confined to the kidney⁷⁶. Thus, it is important to underscore that extrapolation of findings from animal studies to humans is limited.

In humans, the expression of CN1 is distributed among different tissues. Initially, CN1 expression was found in liver and brain and some years later it was reported in the kidney^{76,77,79,90}. Accordingly, Janssen et.al showed an elevated expression in glomeruli of patients with DN and corroborative studies have also shown marked differences in renal CN1 expression between healthy subjects and patients with DN^{77,90}. Peters et. al reported that CN1 is primary localized in the distal tubuli and glomeruli of healthy individuals, while in T2DM patients with DN the expression of CN1 is elevated and much more localized to proximal tubuli⁹⁰.

1.6 Aim of the study

In human both carnosine degrading and synthesizing enzymes, i.e. CN1 and Carnosine synthase (CARNS) are expressed in the kidney. While polymorphisms that are associated with the susceptibility to develop DN have been described for CN1, no such polymorphisms for CARNS have been reported. Therefore the studies performed in the first part of this doctoral thesis particularly focus on the role of CN1 in the progression of DN. Since CN1 is expressed in the kidney and targeted to the secretory pathway we hypothesized that CN1 would be detected in urine as a consequence of renal secretion.

In patients with DN, we expect that the extent of urinary CN1 would be increased as a consequence of impairment in the glomerular filtration barrier integrity.

Because high renal CN1 concentrations may lead to depletion of renal carnosine stores which may have renoprotective properties in hyperglycemic conditions, we also expect an association between the extent of urinary CN1 and renal function deterioration.

The following questions were addressed to test these hypotheses using well-defined patient cohorts:

- 1) Is CN1 found in urine of healthy individuals and in patients with DN?
- 2) Is urinary CN1 associated with renal function deterioration?
- 3) Is urinary CN1 inversely associated with serum CN1 concentrations?
- 4) To what extent is urinary CN1 influenced by the CNDP1 (CTG)_n polymorphism?

Part of the results from this section have been published by Rodriguez-Niño A et al. in *Amino Acids* 51: 17–25, 2019 under the title “*Detection of carnosinase-1 in urine of healthy individuals and patients with type 2 diabetes: correlation with albuminuria and renal function*”.

In the second part of the thesis we performed in vitro experiments to explore the toxicity of MGO towards vascular endothelial cells. We hypothesized that MGO causes structural damage to cultured endothelial cells and that this is ameliorated by carnosine. Because we also expect that MGO affects the redox status in cultured endothelial cells the properties of a roGFP-based redox sensor was tested with the aim to assess how MGO and carnosine affect the intracellular redox milieu in cultured endothelial cells.

To this end the following questions were addressed:

- 5) Does MGO affect viability of endothelial cells and is this counteracted by carnosine?
- 6) Is toxicity by MGO related to DNA damage?
- 7) How is the intracellular redox milieu changed upon MGO and carnosine?

2 MATERIALS AND METHODS

2.1 Materials

2.1.1 Chemicals

2.1.1.1 Commercial chemicals

Table 2. Commercial chemicals

Chemicals	Source
Acrylamide 40 %	Sigma-Aldrich (Germany)
Agarose (PAGE)	Serva (Germany)
Albumin standard (BSA)	Thermo Scientific™ (USA)
Ampicillin	Bioline GmbH (Germany)
APS	Sigma-Aldrich (Germany)
Blue-White Select™ Screening Reagent	Sigma-Aldrich (Germany)
BM blue, POD substrate, soluble	Roche (Germany)
Carnosine (L-)	Sigma-Aldrich (Germany)
CASY-ton	Roche (Germany)
Chemiluminescence Reagent Western Lightning™	Perkin Elmer (USA)
Collagen 0,1%	Sigma-Aldrich (Germany)
Collagenase (from Clostridium histolyticum) Type V	Sigma-Aldrich (Germany)
Coomassie Protein Assay Reagent	Pierce (USA)
DAPI	Sigma-Aldrich (Germany)
Deferoxamine	Sigma-Aldrich (Germany)
DMEM/ high glucose, GlutaMAXGibco®	Thermo Scientific™ (USA)
DMSO	Sigma-Aldrich (Germany)
DnaseI recombinant	Invitrogen (Germany)
DNA ladder buffer 10 x	Invitrogen (Germany)
DNA ladder generuler 1kb	Invitrogen (Germany)
D-PBS 1 x Gibco®	Invitrogen (Germany)
DTT 0,1M	Invitrogen (Germany)
Endothelial cell growth medium, advanced	Provitro (Germany)
Ethanol 100%	Sigma-Aldrich (Germany)
Fetal Calf Serum	PAA Laboratories (Austria)
Gelatin from bovine skin	Fluka (Germany)

Hydrogen chloride 1M	Sigma-Aldrich (Germany)
Hydrogen peroxide 30%	Merck (Germany)
Hydrogen sulfate (H ₂ SO ₄)	Sigma-Aldrich (Germany)
Isopropanol	Merck (Germany)
Laemmli-buffer	BioRad (USA)
LB Agar	Sigma-Aldrich (Germany)
LB Broth Base (Lennox L Broth Base) [®]	Invitrogen (Germany)
Magnesium chloride (MgCl ₂)	Fluka (Switzerland)
2-β-Mercapto ethanol	Sigma-Aldrich (Germany)
Metafectene [®]	Biontex (Germany)
Methanol	Carl Roth (Germany)
Milk powder	Fluka (Switzerland)
Na-butyrate	Sigma-Aldrich (Germany)
NaCl (sodium chloride)	Merck (Germany)
dNTP-Mix (dATP, dTTP, dCTP, dGTP)	Carl Roth (Germany)
PageRuler Plus Prestained Protein ladder	Invitrogen (Germany)
PBS 10x	Invitrogen (Germany)
Penicillin	Sigma-Aldrich (Germany)
Penicillin/streptomycin	Sigma-Aldrich (Germany)
Phosphatase Inhibitor Cocktail	Sigma-Aldrich (Germany)
Poly-D-lysine hydrobromide	Sigma-Aldrich (Germany)
Polybrene	Sigma-Aldrich (Germany)
Protease Inhibitor Cocktail Tablets	Sigma-Aldrich (Germany)
RNase Inhibitor	Roche (Germany)
SDS	Carl Roth (Germany)
TEMED	Sigma-Aldrich (Germany)
Tris/Glycine/SDS buffer 10x	BioRad (USA)
Trichloroacetic acid	Sigma-Aldrich (Germany)
Tris-HCl, Trizma [®] hydrochloride	BioRad (USA)
TRIS buffer 1,5 M (pH =8.8)	BioRad (USA)
Triton [®] X-100	Carl Roth (Germany)
TrypLE [™] Express	Invitrogen (Germany)

Table 3. Chemical preparations

Chemical preparations	Ingredients
APS (for WB)	1g APS add to 10ml ddH ₂ O
Chamber buffer (for WB)	Tris/Glycine/SDS buffer 10x 1:10 diluted in ddH ₂ O
Lysis Buffer	840 µl Lysis buffer Stock 1 µl DTT 10 µl Phosphatase Inhibitor 150 µl Protease Inhibitor
Loading buffer (for WB)	950 µl Laemmli buffer 50 µl β-mercapto ethanol
Lysis buffer, stock solution	10 mM Tris-HCl pH 7.4 150 mM NaCl 5 mM EDTA 1 % Triton X-100 0.5 % Na-Desoxycholat
Lysis buffer, ready to use	840 µl Lysis buffer Stock 1 µl DTT 10 µl Phosphatase Inhibitor 150 µl Protease Inhibitor
MTT reagent	5 mg / ml TBT in PBS
MTT Solution	4 ml 10% SDS 4 ml DMSO 2 ml PBS 1.2% asctetic acid
0.1% PBST (for WB and ELISA)	1x PBS 0.1% Tween20
10 x TBS	12.1g Tris Hcl 87.66 g NaCl add to 1L ddH ₂ O adjust pH value to 8.0
10x Transfer buffer (for WB)	30.3 g Tris, 144.14 g Glycin, add to 1L ddH ₂ O

Fixation solution (for TUNEL)	4% paraformaldehyde in PBS Adjust Ph value to 7.4
Permeabilization solution(for TUNEL)	0.1% Triton X-100 in 0.1% sodium citrate
DNase I recombinant (for TUNEL)	10 μ l DNase I (3000U/ml) 10 μ fetal calf serum 1 ml 50Mm TRIS

2.1.2 Antibodies

Table 4. Antibodies

Antibody	Source	Dilution in WB	Dilution in ELISA
Anti-Human Carnosine Dipeptidase-1 Affinity Purified Polyclonal Ab, Goat IgG (0.2mg/ml)	R&D Systems (Minneapolis, USA)	-----	1:200
Anti-CNDP1 antibody produced in rabbit (ATLAS) polyclonal IgG (0.3 mg/ml)	Sigma-Aldrich (Munich, Germany)	1:1000	1:600
Goat anti-rabbit IgG HRP	Santa cruz (Heidelberg, Germany)	1:2000	1:1000

2.1.3 Restriction enzymes

Table 5. Restriction enzymes

Enzyme	Source
HindIII (for CN1-transgenic mice generation)	New England BioLabs (Germany)
Stu (for CN1-transgenic mice generation)	New England BioLabs (Germany)
XbaI (for roGFP)	New England BioLabs (Germany)
BamHI (for roGFP)	New England BioLabs (Germany)

2.1.4 Primers

Table 6. Primers

Primers	Sequence (5 →3')	Tm (°C)	GC Content (%)
CN1 forward	CCT CGC TTC AGA CAA GAG CTC TTC AGA ATG A	62.4	55
CN1 reverse	GCT CTG AAG GCG CTC ACA GCA TTG ATC CAA	63.8	61.1

2.1.5 Plasmids and vectors

Table 7. Plasmids and vectors

Plasmids and vectors	Source
pMD.G plasmid	kindly offered by Dr. P. Pallavi (Department of Surgery, UMM)
pCMV 8.91 plasmid	kindly offered by Dr. P. Pallavi (Department of Surgery, UMM)
Resen (roGFP)	Genewiz (Germany)
pPm337 vector	Genewiz (Germany)

2.1.6 Kits

Table 8. Kits used in experiments

Kit	Source
DH5α E.coli	Invitrogen (Germany)
Dam- / dcm- Competent E.coli	New England BioLabs (Germany)
Pure Yield Maxi Prep system	Promega (Germany)
Genomic DNA isolation kit	Promega (Germany)
Rapid DNA Ligation Kit	Roche (Germany)
Invisorb spin tissue mini kit	Stratec (Germany)
In situ Cell Death Detection kit, AP	Roche (Germany)
GoTaq® DNA Polymerase Kit	Promega (Germany)

2.1.7 Consumables

Table 9. Plastic and other consumables

Consumables	Source
Cell culture flasks Falcon™ 25 cm ² / 75 cm ²	BD Biosciences (USA)
Disposable cuvettes	Eppendorf (Germany)
Disposable pipette Falcon™ 1 ml/ 2 ml/ 5 ml/ 10 ml/ 25 ml	BD Biosciences (USA)
Disposable scalpel	Feather® (Japan)
Disposable syringes	BD Biosciences (USA)
EDTA-potassium-S-Monovette 2.6 ml	Sarstedt (Germany)
Serum- Monovette 7.5 ml	Sarstedt (Germany)
ELISA, high-binding 96- well plates	Greiner (Germany)
Eppendorf Safe-lock Tubes 0.5 ml / 1.5 ml / 2 ml	Eppendorf (Germany)
Eppendorf epT.I.P.S 0.1-10 µl / 2-200 µl / 50-1000 µl	Eppendorf (Germany)
Falcon™ Tubes 15 ml / 50 ml	BD Biosciences (USA)
Flat bottom plates Falcon™ 6 / 12 / 24 / 96 well	BD Biosciences (USA)
Gel-Blotting-Paper (Filter paper)	Whatman® (England)
Millex®-HA Filter Unit, 33mm (for concentrating virus)	Merck Millipore (Germany)
Mr. Frosty Freezing Container Nalgene™	Thermo Scientific™ (USA)
MultiGuard barrier tips 0.1-10 µl / 2-200 µl / 50-1000 µl	Sorenson Bioscience(USA)
Parafilm® M	Bemis® (USA)
PCR-Tubes™ 0.2 ml	BioRad (USA)
Petri dishes Falcon™	BD Biosciences (USA)
Polyethylen Film, Fisherbrand®	Fisher Scientific (Germany)
PVDF-Membrane	Roche (Germany)
Sterile filter (0.22 µm)	Fisher Scientific (Germany)
VIVASPIN 20	Sartorius stedim (Germany)

2.1.8 Machines and softwares

Table 10. Machines and softwares used for experiments

Machines and softwares	Source
3130 Genetic Analyzer	Applied Biosystems® (USA)
3130 Genetic Analyzer Data Collection Software v. 3.0	Applied Biosystems® (USA)
ABI Prism DNA Analyzer 3100	Applied Biosystems® (USA)
Autoclave Typ ELVC 5075	Systec GmbH (Germany)
Bunsen burner Butane / Propan CV 470 Plus	Campinggaz® (Netherland)
Cell counting CASY®	Schärfe Systems (Germany)
CellF software	Olympus (Germany)
Centrifugation Biofuge Pico/ Fresco/ Primo R	Heraeus (Germany)
Centrifugation 5415/ 5417C	Eppendorf (Germany)
DNA concentration tester (Infinite® 200 NanoQuant)	Tecan (Germany)
DNA Sequencing Analysis Software 5.2	Applied Biosystems® (USA)
Electrophoresis chamber SUB-CELL®-GT	Bio-Rad Laboratories (USA)
Electrophoresis chamber for western blot	Bio-Rad Laboratories (USA)
ELISA Absorption measurement	Tecan (Germany)
GraphPad Prism 7.0	GraphPad Software, Inc (USA)
Guava(easyCyte)	Luminex(USA)
FlowJo	FlowJo(USA)
Imaging system for blot	Biometra (Germany)
Immunofluorescence optical microscopy	Olympus (Germany)
Impulse Sealer	TEW (Taiwan)
Incubator for Cell culture HERAcell 150i	Heraeus GmbH (Germany)
Incubator for bacteria culture	Melag (Germany)
Incubator and shaker Certomat® HK	Biotech International (Germany)
Light microscope DMIL	Leica (Germany)
Microwave oven	Sharp (USA)
Multi-pipette	Eppendorf (Germany)
Pipette	Eppendorf (Germany)
Refrigerator 4 °C	Liebherr (Germany)
Refrigerator -20 °C	Liebherr (Germany)
Refrigerator -80 °C	Liebherr (Germany)
Shaker Vortex-Genie 2	Scientific Industries (USA)
Shaking Incubator	Labnet (England)
Sterile working bench for bacteria culture	Clean Air Supplies (Germany)
Sterile working bench for cell culture	Heraeus (Germany)
Tecan Spark M10 with injector	Tecan (Germany)

Thermoblock TechneDri-Block® DB-2D	Biostep GmbH (Germany)
TransBlot turbo	Bio-Rad Laboratories (USA)
UV Light 312 nm and CCD camera System	Intas (Germany)
Vacuum system for maxiprep	Promega (Germany)
Vortex machine 120	Heidolph (Germany)
Water bath Typ 3043	Köttermann (Germany)
Weight balance	Sartorius (Germany)
Western-Blot imaging system Chemismart 5100	PEQLAB (Germany)
XL STAT Biomed	Addisoft (USA)

2.2 Methods

2.2.1 Participant recruitment and sampling

Living kidney donors and patients with T2DM (DIALECT cohort)

Participants:

A total of 361 T2DM patients from the DIALECT cohort were included in this study. DIALECT is a prospective study of T2DM patients recruited in ZTD (Ziekenhuisgroep Twente) a secondary health care center in the Netherlands⁹¹. The study was approved by the local institutional review boards of the Netherlands (METc-registration numbers NL57219.044.16 and 1009.68020) and is registered in the Netherlands Trial Register (NTR trial code 5855). Patients with type 2 diabetes older than 18 years old, able to understand the informant consent were eligible. Patients that underwent kidney transplantation or patients with dependency on renal replacement therapy were excluded.

The living kidney donors patients (control group) consisted of 243 healthy individuals that were regularly checked for living kidney donation in the University Medical Center Groningen. None had medical history of diabetes, kidney or cardiovascular disease. The institutional board approved the study protocol (METc 2008/186).

Sampling and definitions:

For the 24-h urine collection, patients were instructed to dispose of the first morning void urine, and thereafter collect all urine in a provided container until the first urine of

the next day. Albuminuria, glycosuria and urinary CN1 excretion rates were calculated by multiplying concentrations with the volume of the 24-h urine collection. Normoalbuminuria was defined as 24-h urinary albumin excretion of <30mg/day. Micro and macroalbuminuria were defined as 24-h urinary albumin excretion of 30-300 mg/day and >300 mg/day respectively. Estimated glomerular filtration rate (eGFR) was calculated according to CKD- EPI formula. Tests for assessing HbA1c, serum creatinine and cholesterol were performed in venous blood.

Mannheim cohort

Participants:

Patients were recruited in the Vth Medical Clinic and in the Dialysis Unit at the University Medical Centre Mannheim. A total of 111 patients were included in the study and allocated in 2 groups: i.e. patients with type 2 diabetes and chronic kidney disease (n=85) and non-diabetic patients with other causes of kidney injury (CKD) (n=26). For allocation in the T2DM group patients met the following criteria: diabetes mellitus known from medical history and/or diagnosed by HbA1c >6.5% levels or fasting glucose >126 mg/dl.

Non-diabetic patients with CKD were included after screening of patient medical records, medications and laboratory testing for plasma glucose or HbA1c to exclude diabetes. All patients were sub grouped according to their kidney function and degree of albuminuria.

Sampling and definitions:

Persistent albumin excretion in at least 2 independent occasions of >200 mg/l or ACR ratio (albumin/creatinine ratio) >300 mg/g was considered as macroalbuminuria. Microalbuminuria and normoalbuminuria were defined as ACR: 30-300 mg/g and ACR<30 mg/g respectively in at least 2 independent occasions.

Parameters including glycated hemoglobin (HbA1c) body mass index (BMI), serum creatinine, and albuminuria/creatinine ratio (ACR) were extracted from medical records. Estimated glomerular filtration rate (eGFR) was calculated according to CKD- EPI formula. Patients that underwent kidney transplantation or patients without residual diuresis were excluded. Subjects with missing urine and blood sampling were also excluded. The healthy controls consisted of 25 adults (17 females and 8

males) members of our laboratory staff or students that voluntarily decided to participate. None of them had history of diabetes, cardiovascular or kidney disease. The study was approved by the ethical committee and relevant local institutional review boards (193/2001). All patients and healthy volunteers enrolled in the study gave their written informed consent.

Spot urine samples were collected by spontaneous miction and stored in -20 until further analysis. For measurement of plasma carnosinase concentration and CN1 genotyping, blood of the antecubital vein was withdrawn and stored in -20 until processing.

All procedures performed in studies involving human participants were in accordance with the ethical standards of the institutional and national research committee and with the 1984 Helsinki declaration and its later amendments or comparable ethical standards

2.2.2 ELISA assays

CN1 concentrations in serum and urine were measured by ELISA as previously described by Adelman et. al respectively⁹². Briefly, High-binding microtiter plates were coated overnight with 100 µl of goat polyclonal anti-human CN1 (10 µg/ml). The plates were extensively washed and incubated with 0.05% of dry milk powder to avoid unspecific binding. Serum samples were tested in a dilution of 1:100 or 1:200 and urine samples were tested undiluted. Each sample was tested in duplicate. The plates were placed on a shaker for 1 hour and subsequently washed with 1x PBS/Tween. Thereafter, rabbit polyclonal antibody (ATLAS, Abcam plc, Cambridge, United Kingdom) was added for 1 hour followed by extensive washing. Goat anti-rabbit IgG HRP-conjugated antibody was added for 30 min followed by extensive washing. Deep-blue peroxidase (POD) (Roche diagnostics, Mannheim, Germany) was used for color development and reaction was stopped after 15 min by the addition of 50 µl of 1 M H₂SO₄. The plates were directly read at 450 nm fluorescence. A serial dilution of pooled serum with a known concentration of carnosine (2µg/µl) was used as standard. CN1 protein concentrations were assessed in the linear part of the dilution curve with a lower detection limit of 31 ng/ml. Concentrations below the detection limit were considered as CN1 negative or zero.

2.2.3 CN1 enzymatic activities

CN1 activities in urine and in recombinant protein were measured as described by Peters et al 2010. Briefly, reaction was initiated with addition of carnosine into the samples and stopped with 1% trichloroacetic acid at predetermined time points (0- 5- 15 and 30 minutes). Supernatants were taken after centrifugation and placed in a new tube in combination with o-Phthalaldehyde. Fluorescence liberated by histidine substrate was read using a Tecan plate reader ($\lambda_{\text{Excitation}}$: 360 nm; $\lambda_{\text{Emission}}$: 460 nm).

2.2.4 Generation of hCN1 transgenic mice

Briefly, the cDNA of human CN1 including the endogenous signal peptide of six leucines was amplified from IMAGE clone acc.no.BX094414 using the primers CN1 forward 5'PCACCATGGATCCCAAACCTCGGGA3' and CN1 reverse 5'PTCAATGGAGCTGGGCCATCT3'. PCR product was ligated into the Stu1 site of plasmid pTTR1ExV3 which contains the transthyretin promoter and drives hCN1 expression specifically within the liver and brain. After fragment digestion using HindIII, the purified fragment was injected into the pronuclei of the fertilized ovum of BTBR (Black and Tan, BRachyuric) female mouse (purchased from Jackson Laboratories, Bar Harbor, ME, USA). All animal procedures were approved by the Regierungspräsidium Karlsruhe (AZ 35-9185.81/G-116/14).

2.2.5 DNA isolation and sampling for animal experiments

DNA was isolated from mice tails by making use of the Invisorb spin tissue mini kit according to the manufacturer's instructions. The transgene TTP-hCN1 mutation was genotyped by PCRs as described in Sauerhöfer et. al ⁶⁴. Mice were housed at 22° C in a 12h light/dark cycle and fed regular chow and water ad libitum. At week 24 of age, blood samples were collected from the orbital plexus under anesthesia and serum was isolated by centrifugation. To obtain morning spot urine samples, animals were placed in metabolic cages at the beginning of the light cycle. Samples were stored at -20 until further use. Serum and urinary CN1 concentrations were assessed with ELISA as previously described.

2.2.6 CNDP1 genotyping

Animal experiments

PCR assays were performed to ensure the integration of human CN1 gene.

Briefly, PCR was performed using primers CN1 forward 5'CCTCGCTTCAGACAAGAGCTCTTCAGAATGA3' and CN1 reverse 5'GCTCTGAAGGCGCTCACAGCATTGATCCAA3' yielding a product of 343 base pairs. The PCR application program is depicted as follows:

	T°	Duration	Step	
1	94 °C	3 minutes		30 cycles
2	94 °C	1 minute	Denaturation	
3	60 °C	45 seconds	Annealing	
4	72 °C	2 minutes	Extension	
5	72°C	10 minutes		
6	4° C	∞	End of cycle	

Human participants

Genomic DNA was isolated from EDTA blood using the Genomic DNA isolation kit (Promega, Mannheim, Germany). A standard PCR protocol with the following fluorescence labeled forward primer: 5'-FAM-GCGGGGAGGGTGAGGAGAAC-3' and unlabeled reverse primer 5'GGTAACAGACCTTCTTGAGGAATTTGG-3 was used.

After PCR amplification, fragment analysis was performed with an ABI310 analyzer (Perkin Elmer) to determine the fragment length corresponding to the different genotypes. Each peak corresponded with the number of leucine repeats(CTG)_n on each allele. The 157-, 160-, and 163-bp products corresponded with (CTG)₅, (CTG)₆, and (CTG)₇ repeats, respectively.

2.2.7 Protein precipitation and Westernblotting

Qualitative detection of CN1 by Westernblotting was performed as previously described ⁹². Urine samples from healthy subjects were approximately 10x

concentrated. Protein precipitation was performed by addition of 1 volume of 100% Trichloroacetic acid to 4 volumes of sample and supernatants were removed after centrifugation. Pellets were washed twice with 200 μ l of cold acetone and let dry for 10 minutes in 95°C heat block. Pellets were dissolved in laemmli sample buffer containing β -mercaptoethanol and boiled for 20 minutes. Urine and serum samples were loaded on a 10% SDS-PAGE gel and run at 180V for 1 hour. Proteins were transferred to a PVDF membrane by semi-dry blotting at 1A/25V for 30 mins. The membrane was blocked with 5% milk powder in 1% TBST for 1 hour and thereafter incubated with primary antibody diluted in 5% milk powder at 4°C overnight. Next day membrane was washed three times with TBST and incubated for 1 hour with the corresponding secondary antibody. After extensive washing detection of immune reactive bands was performed by enhanced luminol reagent and visualized by chemiluminescence.

2.2.8 HUVECs isolation

Fresh umbilical cords were obtained from the obstetric department of UMM. Permission to isolate endothelial cells from umbilical cords was granted by the medical ethics committee of the medical faculty Mannheim (AZ 2015-518N-MA). Human umbilical vein endothelial cells (HUVECs) were isolated by insertion and fixation with suture thread of glass tubes into both ends of the umbilical vein. The veins were flushed with 20ml PBS twice to remove erythrocytes. Thereafter, sterile collagenase solution (0.5mg/ml in PBS) was injected into the vein, followed by 12 minutes of incubation in water bath at 37°C. The collagenase solution was transferred to a new 50ml falcon tube by flushing the vein with 20 ml of 10% FCS and PBS. The cells were centrifuged (300g, 5min), re-suspended in medium, and transferred to a previously coated-T25 flask.

2.2.9 Cell Culture

HUVECs were cultured in endothelial cell growth medium (Provitro, Berlin, Germany) containing 7.5% FCS and 50ng/ml amphotericin B together with 50 μ g/ml gentamicin 37°C and 8% CO₂. The flasks for HUVECs were coated in 1% gelatin 20 min before

use. All experiments involving HUVECs were performed in passages 2-6. HEK293 and H1080 cells were cultured in DMEM high glucose GlutaMAX (Thermo fisher) containing 10% FCS and penicillin (100U/ml) / streptomycin (100µg/ml) in an incubator at 37°C and 5% CO₂.

2.2.10 Cell viability assay

HUVECs were seeded at different densities in 96 well plates. Next day cells were challenged with different concentrations of Methylglyoxal for 24 hours and toxicity was assessed by MTT assay. Briefly, 200µM thiazolyl blue tetrazolium bromide (5mg/ml in PBS) dissolved in cell medium (1:10) was added into each well. Cells were placed in incubator at 37 °C for 4-5 hours. Hereafter, crystals of formazan were dissolved by the addition of 100µM MTT solvent. The cells were incubated overnight at 37 °C. Absorbance was measured at a wavelength of 560 nm, using 670nm as a reference wavelength. Cell viability was calculated as percentage relative to untreated cells.

2.2.11 DNA damage assay

Following treatment with Methylglyoxal, cells were fixated with 4% paraformaldehyde and air dried for 1 hour. Thereafter, cells were incubated with permeabilisation solution for 2 minutes on ice and rinsed with PBS. To induce DNA strand breaks some cells were treated with Dnal recombinant (3000u/ml) for 10 minutes and used as a positive control. For the negative control only label solution was added.

After drying, 50µL of TUNEL reaction mixture was added and cells were incubated for 1 hour at 37°C in a humidified atmosphere in the dark. Hereafter cells were rinsed with PBS and labeled with DAPI (1:5000) for 30 mins for nuclei visualization. After extensive washing cells were analyzed under fluorescence microscopy.

2.2.12 Subcloning of roGFP and lentivirus production

Constructs were designed by Dr. Prama Pallavi and synthesized by Genewitz (Clone ID B32523-1/q28382). The constructs were generated by fusing the coding sequences of human Grx1 with roGFP and thereafter subcloned into the pPM337

lentiviral vector. For the production of lentivirus containing roGFP, HEK293T cells were transfected with a HIV-based 3-plasmid system (pCMV8.91, pMD.G and the plasmid containing roGFP). Supernatants were concentrated as viral particles.

2.2.13 Lentivirus transduction and titration

Before vector infection of our target cells (HUVECs), transduction efficiency was examined by incubating HT1080 cells for 48 hours with different concentrations of lentiviral particles. Percentage of GFP positive cells was determined by FACS with Guava easyCyte using 488nm laser line for excitation and 525/30 nm filter set for emission. Data were analyzed using FlowJo software and used to calculate virus titer in each dilution. Cells were also visualized under fluorescence microscopy (10x) (**Fig. 3 A**). HUVECs were transduced with different concentrations of lentiviral vector for 48 hours and transduction efficiency was assessed by visualization of GFP under fluorescence microscopy (40x) (**Fig.3 B**).

Since in transduced HUVECs an optimal expression of GFP was observed at 1:100 dilution, this lentiviral concentration was used in posterior experiments. The stability of the vector over passages was also verified by qualitative assessment of GFP under the fluorescence microscope. Up to three passages after transduction no evident GFP expression changes were observed (data not shown).

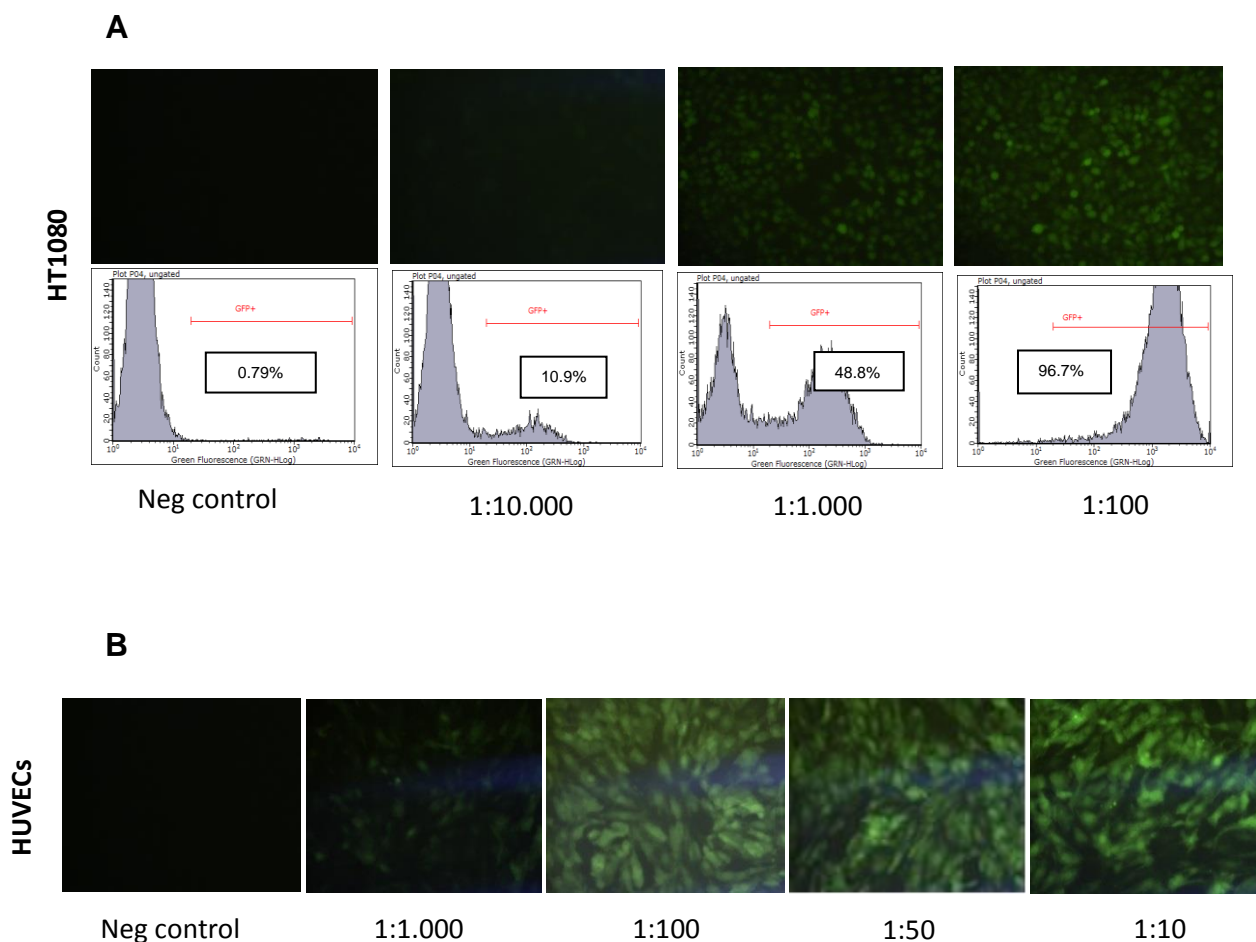


Fig. 3 Transduction of cells with roGFP-containing lentiviral vector. (A) HT1080 cells were incubated with different concentrations (1:100 to 1.10.000) of lentiviral particles containing roGFP (GFP-coupled redox sensor). Vector integration was assessed by FACS and fluorescence microscopy. At a 1:100 dilution positivity of nearly all the cells (96.7%) by FACS analysis is observed. **(B)** HUVECs were incubated with 1:10 to 1:1000 dilution of lentiviral particles. Note that at 1:100 a strong positivity for GFP is observed under fluorescence microscopy, magnification (40x).

2.2.14 Radiometric measurements

RoGFP expressing cells were seeded in 96-well plate. Next day, prior to measurements cell medium was exchange with PBS. We measured the emission of roGFP at 528nm after excitation at 395 and 485 nm in a plate reader set at 37°C (Tecan Spark M10) equipped with built-in injectors.

2.2.15 Statistical analysis

Continuous variables were expressed as means \pm SD or median and interquartile range (IQR). Categorical variables were expressed as numbers and percentages. For comparison of groups, independent two tailed Student's t-test or ANOVA with Tukey's were applied for continuous variables if normally distributed. For data with skewed distribution Mann Whitney-U or Kruskal-Wallis test with Dunn's test were applied. For the analysis of categorical variables Fisher's test or χ^2 with bonferroni correction (based on the number of comparisons) were applied.

Variables with skewed distribution i.e. urinary CN1, serum CN1, glycosuria and albumin/creatinine ratio (ACR) were log-transformed and correlations with other continuous variables were assessed using Pearson correlation test.

Backward and Forward stepwise regression analysis were employed with log-transformed urinary CN1+1 as a dependent variable to determine the best multivariate model predicting urinary CN1 concentrations. All statistical tests were two-sided and a p value <0.05 was considered statistically significant in all analyses. The analyses were assessed with Graph Pad Prism version 7.02 and XLSTAT

3 RESULTS

3.1 Detection of Carnosinase1 in urine

Carnosinase1 (CN1) is predominantly produced by the brain and by the liver from where it is secreted into the circulation. Based on recent findings suggesting that CN1 is expressed in human kidney and that the signal peptide within CN1 enables its secretion, this study was carried out to assess whether CN1 can be detected in urine. Firstly, we assessed whether our *in-house* developed ELISA system used for CN1 detection in serum or plasma was also suitable for the detection of CN1 in urine samples. To this end, serial dilutions of known concentrations of CN1 recombinant protein (rCN1) were made in spot urine samples from healthy individuals or in standard diluent (phosphate buffer saline) respectively.

The spike-recovery of the assay was calculated by comparing the detected and expected concentrations of rCN1 in the different dilution points. Optimal spike recoveries were observed for both matrices with an average spike recovery of 109% which is within the acceptance range (80-120%) and suggests that urine matrix components do not interfere with or inhibit CN1 detection. The detection range of the ELISA was 31 ng/ ml up to 2000 ng/ml and linearity of the curves was observed in a concentration range of 100 to 1000 ng/ml (rCN1 spiked in urine : $R^2 = 0.99$; rCN1 spiked in PBS: $R^2 = 0.97$) (**Fig.4A**)

The specificity of the in-house developed ELISA system was assessed by testing urine and serum samples of mice overexpressing human CN1 (hCN1 transgenic mice) and wild type mice.

As depicted in **Fig. 4B**, CN1 was exclusively detected in mice overexpressing the hCN1 transgene and was undetectable in wild type mice. The presence of CN1 in serum and urine from mice was further verified by Westernblotting (**Fig.4C and 4D**)

To further characterize the presence of CN1 in urine we assessed whether naturally occurring CN1 in human urine has any enzymatic activity.

Although no enzymatic activity was detected in any human urine sample or in urine from CN1 transgenic mice, the addition of rCN1 to human urine resulted in measurable activities nearly comparable to that of rCN1 in standard assay buffer (**Fig.4E**).

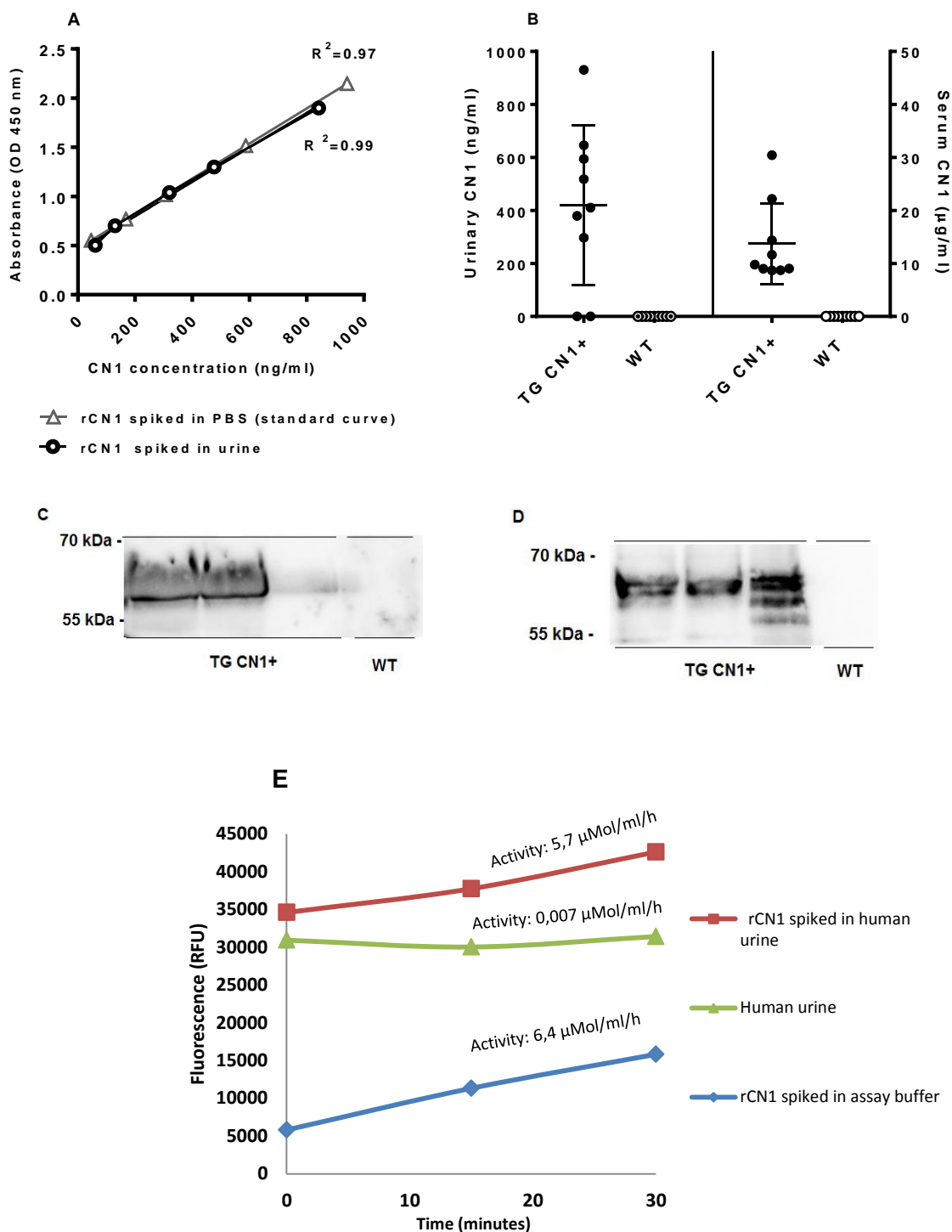


Fig.4 Detection of CN1 (A) Recombinant CN1 (rCN1) was spiked in human urine or standard diluent (PBS). CN1 was detected by ELISA in serial dilutions using urine or PBS as diluent. (B) Specificity of the ELISA system: CN1 concentrations in serum (right y axis) and in urine (left y axis) of transgenic mice overexpressing human CN1 (TG CN1+) (n=9) and wild type mice (WT) (n=9). Representative Westernblotting of CN1 in serum (C) and urine (D) from transgenic CN1+ and wild type mice. (E) Human urinary CN1 displays no enzymatic activity whereas enzymatic activity of rCN1 spiked in human urine is measurable. Enzyme activity was measure as degradation of carnosine and derivation of the free amino acids as described in the methods.

3.2 Characterization of 24h urinary CN1 in living kidney donors and T2DM patients (DIALECT cohort)

During the validation of the ELISA system, we noticed that the blanks, i.e., urine without spiked CN1, showed traces of CN1 in the samples of some individuals. To substantiate these findings and to assess to what extent CN1 is detected in urine, 24h urine samples of living kidney donors (n= 243) and patients with T2DM (n = 361) were collected and screened for CN1. Demographic characteristics of T2DM stratified by albuminuria excretion rate into normoalbuminuria (albuminuria>30 mg/24h) (n=241), microalbuminuria (albuminuria 30-300 mg/24h) (n=80) and macroalbuminuria (albuminuria >300 mg/24h) (n=40) are displayed in Table1.

Table 11. Demographic and clinical characteristics of T2DM related to albuminuria.

Characteristics	T2DM			p value
	Normo-albuminuria n = 241	Micro-albuminuria n=80	Macro-albuminuria n= 40	
Demographic				
Men, n(%)	118(49)	56(70) [#]	31(78) [#] [§]	0.016
Age (years)	62.8 ± 8.8	63.6 ± 9.0	67.5 ± 7.9 [#]	0.007
Clinical				
SBP (mm Hg)	134.6 ± 15.3	139.4 ± 16.8	140.3 ± 19.4 [#]	0.002
DBP (mm Hg)	74.1 ± 9.0	75.3 ± 10.3	75.2 ± 10.8	0.55
Body mass Index (kg/m ²)	32.7 ± 6.0	33.0 ± 5.7	32.8 ± 6.1	0.75
Duration of diabetes (years)	11[6 - 18]	12[6 -18]	10[6 -19]	0.65
Retinopathy, n(%)	55(22)	26(33)	11(28)	0.21
HbA1c (%)	7.3 ± 1.0	7.6 ± 1.2	7.2 ± 1	0.16
Kidney Function				
Serum creatinine (mg/dl)	0.9 ± 0.3	1.1 ± 0.6 [#]	1.4 ± 0.5 [#] [§]	<0.0001
eGFR (ml/min/ 1.73 m ²)	81 ± 22	75 ± 26	54 ± 22 [#] [§]	<0.0001
Urine Osmolarity (mOsm/kg)	486.8 ± 210.0	494.6 ± 217.9	415.0 ± 170.4	0.10
Urine Volume (ml)	2024 ± 783	2071 ± 775	2153 ± 961	0.48
Glycosuria (mg/24 h)	451[85- 5263]	1137[105 – 8393]	326[74 – 4349]	0.17
Albuminuria (mg/24 h)	4.4[1.5 – 11.1]	82.4 [59.6 –145.8] [#]	508.0[365.4 – 900.1] [#] [§]	<0.0001
ACEi/ARB, n(%)	158(63.5)	57(71.4)	34(85) [#]	0.016

p values were calculated using one-way ANOVA, Kruskal Wallis or Chi² with Bonferroni correction.

[#]: compared to patients with normoalbuminuria, [§]: compared to patients with microalbuminuria.

In the group of patients with macroalbuminuria, the proportion of males was higher. The patients in this group were also older, showed higher levels of systolic blood pressure, higher serum creatinine concentrations and lower eGFR in comparison to patients with normo- and microalbuminuria. Additionally, a higher proportion of patients on ACEi/ARB therapy were found in the macroalbuminuric group compared to the other two groups (**Table. 11**).

The proportion of CN1 detected in urine samples of macroalbuminuric patients was significantly higher (39 of 40) compared to the groups with microalbuminuria (65 of 80) and normoalbuminuria (147 of 241) (97% vs 81% vs 63.5%, $p=0.016$) (**Fig.5 A**).

In the healthy group, urinary CN1 was detected in 180 of 243 subjects (74%) (data not shown) The presence of CN1 in urine from T2DM patients and living kidney donors was qualitatively assessed by Westernblotting. (**Fig. 5 B and 5 C**)

The median urinary CN1 excretion rates were significantly higher in patients with macroalbuminuria when compared to the micro- and normoalbuminuria groups (1.5 mg/24h [IQR, 0.5 – 3.8 mg/24h] vs 0.2 mg/24h [IQR, 0.08 – 0.8 mg/24h] vs 0.1 mg/24h [IQR, 0 – 0.4 mg/24h]; $p < 0.0001$). Likewise, microalbuminuric patients displayed higher CN1 excretion rates in comparison to the group with normoalbuminuria ($p < 0.05$) (**Fig. 5 D**).

In the living kidney donors median CN1 excretion rates were: 0.2 mg/24h [IQR, 0 – 0.6 mg/24h] and compared to T2DM patients significant differences were only found with the macroalbuminuric group. ($p < 0.0001$) (**Fig. 5 D**).

To better understand the relation between urinary CN1 and renal function, we looked at urinary CN1 concentrations in T2DM patients stratified on the basis of estimated glomerular filtration rate (eGFR) in <30 , $30-60$ and >60 ml/min/1.73m². As depicted in **Fig.5 E**, patients with severely impaired renal function (<30 ml/min/1.73m²) appeared to have higher concentrations of urinary CN1 concentration in comparison to patients with preserved renal function (>60 ml/min/1.73m²).

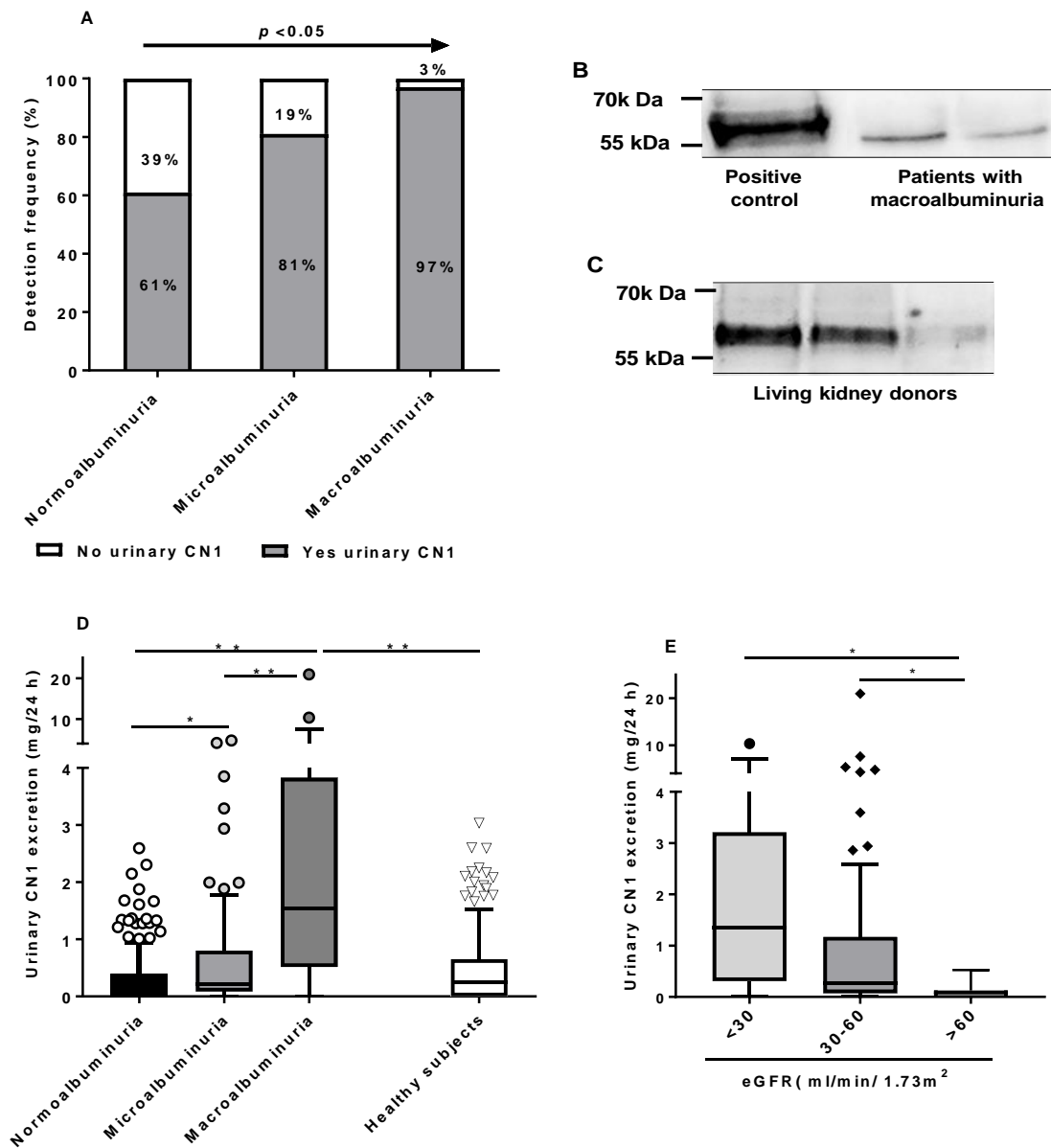


Fig.5 (A) Proportion of urinary CN1 detection in T2DM patients stratified according to normo-micro- and macroalbuminuria. **(B)** Westernblotting of CN1 in urine obtained from 2 diabetic patients with macroalbuminuria. Positive control: urine from CN1+ transgenic mouse. The samples were loaded without prior concentrating of the urine. **(C)** Detection of CN1 in 10x concentrated urine from 3 healthy individuals by Western Blotting. The bands are in concordance to the molecular weight of monomeric CN1. **(D)** Distribution of urinary CN1 concentrations in T2DM stratified according to albuminuria and in healthy subjects. **(E)** Distribution of urinary CN1 in T2DM according to eGFR. Patients were stratified into those with impaired (eGFR<30 ml/min/1.73m²) (n=13), intermediate (eGFR 30-60 ml/min/1.73m²) (n=74) and preserved renal function (eGFR >60 ml/min/1.73m²) (n=273); Boxes and whiskers represent the median and IQR. Outliers are indicated by circles. * $p < 0.05$, ** $p < 0.0001$.

To investigate the association of urinary CN1 with clinically relevant parameters in diabetes we performed correlation analyses. In line with the aforementioned results, urine CN1 excretion rates were found to be positively and significantly associated with albuminuria ($r = 0.59$, $p < 0.0001$) (**Fig.6 A**). There was a modest negative correlation between CN1 excretion rates and eGFR ($r = -0.24$, $p < 0.0001$) (**Fig. 6 B**). Additionally, there was a significant, albeit weak positive correlation between urinary CN1 excretion rates and glycosuria ($r = 0.13$, $p = 0.017$) (**Fig. 6 C**).

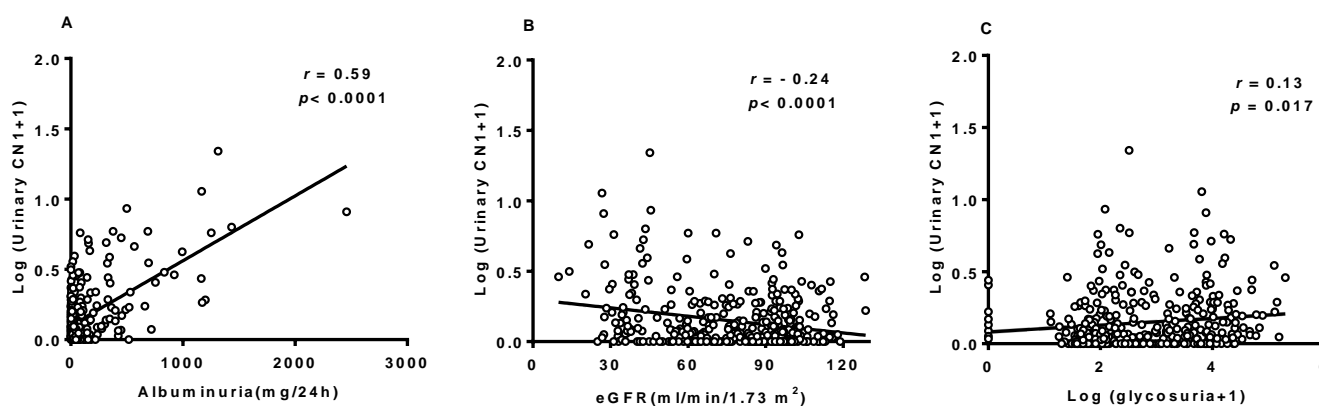


Fig.6 Significant correlations between urinary CN1 and clinical parameters in T2DM patients.

(A) Positive correlation between urinary CN1 (log (urinary CN1+1)) and albuminuria, **(B)** Inverse correlation between urinary CN1 (Log (urinary CN1+1)) and eGFR. Positive correlation between urinary CN1 (Log (urinary CN1+1)) and glycosuria

In order to assess the independent influence of these factors on urinary CN1 a backward stepwise multivariate linear regression analysis was conducted. Urinary CN1 excretion rate was set as the dependent variable and its values were log transformed due to a skewed distribution (Log CN1+1). As shown in **Table 12.**, albuminuria, eGFR, and glycosuria, appeared to be the best explanatory factors of Log CN1 excretion rates. All together, these parameters explain 37% of changes in urinary CN1 excretion rates ($R^2 = 0.37$; $p < 0.0001$).

Table 12. Multivariate linear regression analysis in T2DM patients

Predictive Parameter	Beta Value	95% CI	p value
eGFR(ml/min)	-0.001	-0.002 – -0.00015	0.019
Log (glycosuria excretion + 1)	0.014	0.016 – 0.048	0.0007
Albuminuria (mg/24 h)	0.0004	0.0004 – 0.0005	< 0.0001

Variables predicting urinary CN1 excretion rates (log (urinary CN1+1)) in patients with T2DM. Goodness of fit of the full model: $R^2 = 0.37$, $p < 0.0001$, CI: confidence interval.

3.3 Association of serum CN1 and CNDP1 genotype with urinary CN1 in patients with T2DM and non-diabetic CKD.

Although 24h urine collection has been considered the gold standard for the assessment of albuminuria, it is not routinely performed since it can be time-consuming and often inaccurate due to frequent collection errors. Hence, in large cohorts and biorepositories mostly spot urine samples are collected. Based on this, we assessed if urinary CN1 can also be reliably detected in spot urine and if so, to confirm its association with renal function and albuminuria. Additionally, we examined whether the (CTG)₅ polymorphism within the CNDP1 gene influences urinary CN1 concentrations.

To this end, CN1 metabolism, i.e. CN1 in serum, CN1 in spot urine and CNDP1 (CTG)_n genotype was studied in healthy subjects (n=25), patients with T2DM (n= 85) and in patients with CKD of non-diabetic etiology (CKD) (n=26). The baseline characteristics of T2DM and CKD stratified by microalbuminuria (ACR≤300 mg/gr) and macroalbuminuria (ACR>300 mg/gr) and the healthy subjects are depicted in **Table 13**.

T2DM Patients with macroalbuminuria (ACR>300mg/gr) showed higher diabetic retinopathy frequencies, higher serum creatinine and lower eGFR levels compared to T2DM patients with microalbuminuria (ACR≤300mg/gr). CKD patients with macroalbuminuria displayed increased serum creatinine and low eGFR levels in comparison to CKD patients with microalbuminuria but these did not reach statistical significance (**Table 13**). The main causes of CKD of non-diabetic etiology were Ig-A nephropathy, focal glomerular sclerosis and glomerulonephritis.

Noteworthy, in the overall patient cohort (T2DM and non-diabetic CKD) (n=111), only 18% of the patients had normoalbuminuria (ACR<30 mg/gr), less than 14% (16 of 111) of patients showed eGFR above 60 ml/min/1.73m² and 41% (46 of 111) were on renal replacement therapy. These characteristics reflect a population with predominant kidney impairment.

The healthy control group consisted of 25 healthy adults without clinical signs or medical history of renal disease or diabetes. In this group there were more females (68%) than males and they were significantly younger (mean: 30 ± 9.3 years) compared to both disease groups (p<0.0001) (**Table 13.**)

Urinary CN1 was detected in 95% of T2DM patients with macroalbuminuria and in 48% of patients with microalbuminuria (p<0.0001). Likewise, the proportion of CN1 detection in urine from CKD patients with macroalbuminuria was higher compared to the CKD group with microalbuminuria (88% vs 33%; p=0.0007) (**Table 13.**). In the healthy group, CN1 in spot urine was detected in 18 of 25 subjects (72%)(**Table 13.**)

The concentrations of urinary CN1 were higher in macroalbuminuric in comparison to microalbuminuric patients irrespective of the baseline disease (T2DM: 554 ng/ml [IQR 212-934 ng/ml] vs 0 ng/ml [IQR 0-63.5 ng/ml] p<0.0001; CKD: 197.1 ng/ml [IQR 112.1-738.5] vs 0 ng/ml [IQR 0-226 ng/ml] p=0.015) (**Fig. 7 A**). In the healthy group median urinary CN1 concentrations were: 77 ng/ml [IQR 0- 118.5] and were significantly lower compared to T2DM (p<0.0001) and CKD patients with macroalbuminuria (p=0.004) (**Fig. 7 A**). In line with these findings, a positive correlation between albuminuria (ACR) and urinary CN1 concentrations was found in the overall cohort of patients (r=0.66, p<0.0001) (n=111) (**Fig. 7 B**).

Furthermore, when patients were stratified on the basis of renal function into eGFR <60 vs. eGFR >60 ml/min/1.73m², significantly higher urinary CN1 concentrations were found in patients of the lower eGFR strata (p<0.05) (**Fig. 7 C**)

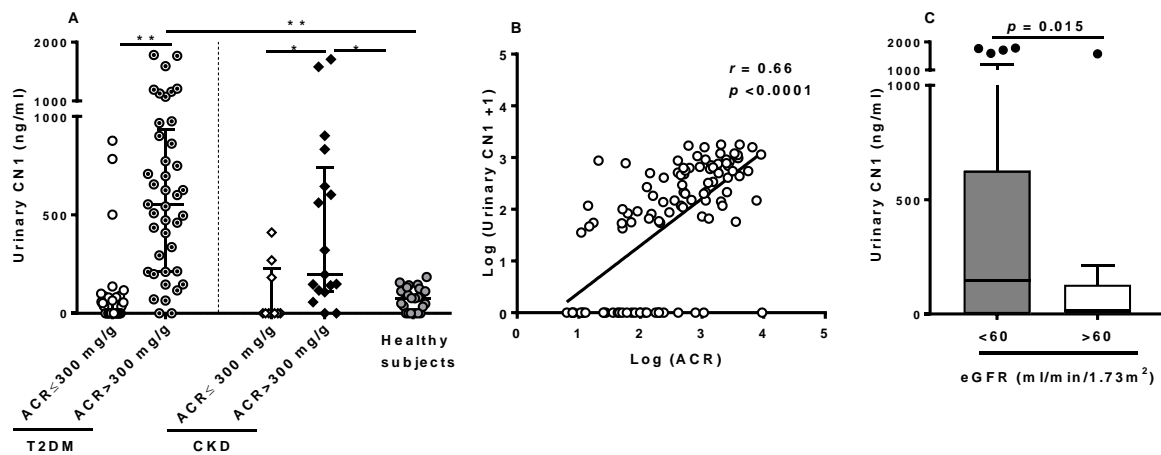


Fig. 7 (A) Distribution of CN1 in spot urine of T2DM and non-diabetic patients (CKD) with microalbuminuria ($ACR \leq 300 \text{ mg/g}$) and macroalbuminuria ($ACR > 300 \text{ mg/g}$) and healthy subjects. Results are expressed for each individual patient. The lines represent the median and IQR. **(B)** Pearson correlation between ACR (Log (ACR)) and urinary CN1 concentrations ($\text{Log (urinary CN1+1)}$) in patients with T2DM and in non-diabetic patients ($n=111$). **(C)** Distribution of urinary CN1 concentrations in all patients according to eGFR. T2DM and CKD patients ($n=111$) were stratified according to poor ($eGFR < 60 \text{ ml/min/1.73m}^2$) ($n= 95$) and preserved renal function ($eGFR > 60 \text{ ml/min/1.73m}^2$) ($n= 16$). Boxes and whiskers represent the median and IQR. Outliers are indicated with circles.

Table 13. Demographic and clinical characteristics of T2DM and non-diabetic CKD related to ACR and healthy subjects

Characteristics	T2DM		p value	CKD		p value	Healthy subjects n=25
	ACR<300 mg/g n= 44	ACR≥300mg/g n=41		ACR<300 mg/g n=9	ACR≥300 mg/g n=17		
Demographic							
Male sex n (%)	27(61)	30(73)	0.24	7 (78)	9(53)	0.39	8(32)
Age(years)	68.3 ± 15.1	62.4 ± 15	0.06	70 ± 16.3	65.8 ± 17.9	0.61	30 ± 9.3
Clinical							
Body mass Index(kg/m ²)	31.3 ± 7.3	30 ± 6.3	0.28	28 ± 3.9	29 ± 6.8	0.68	
Hba1c (%)	8.2± 2.4	7.6 ± 2.0	0.22	5.1 ± 0.5	5.4 ± 0.8	0.31	
Serum Albumin(gr/l)	28.7±7.5	27.8±6.6	0.56	29.2±4.7	29±5.9	0.93	
FPG (mg/dl)	154.5± 66.2	145± 64	0.50	96.3 ±10.3	90 ±11	0.15	
Systolic BP(mmHg)	134.3 ± 22.4	142.5 ± 16.8	0.06	131.2 ± 26.2	137.7 ±19.4	0.48	
Diastolic BP(mmHg)	74.1±13.1	75.3±15.1	0.72	72±13	76.3±15.8	0.50	
Diabetic Retinopathy n(%)	19(43)	31(75)	0.004	-	-		
Kidney Function							
Serum creatinine(mg/dl)	2.5 ± 1.7	4.7 ± 3.3	0.002	3.8 ± 2.0	4.4 ± 3.1	0.58	
eGFR(ml/min/1.73m ²)	33 [17 - 60]	13 [7.5 – 30]	0.0005	12.6[8.3 – 49.4]	11.9[7.9 - 32]	0.80	
Albuminuria ACR(mg/g)	49.5 [13.3 -112]	1498 [580 - 3261]	<0.0001	127 [31 – 207.5]	1150 [641.5-2099]	<0.0001	
Dialysis n(%)	13 (30)	20 (49)	0.08	4 (44)	9 (53)	0.68	
- Hemodialysis n(%)	12	18		4	9		
- Peritoneal dialysis n(%)	1	2		-	-		
Residual diuresis(ml/24h)	1600 [850-2500]	1000[650-2000]	0.09	1500[750-2000]	1500[1000-1572]	0.97	
Pharmacological management							
ACEi/ARB n(%)	25(57)	25(61)	0.70	4(44)	9(53)	0.68	
Diuretic n(%)	30(68)	29(71)	0.80	7(78)	12(71)	0.69	
CN1 metabolism							
CN1 in serum (µg/ml)	3.9 [2.1 – 12]	4.6 [2.6 – 12.2]	0.74	3.0 [1 - 4.6]	3.9 [0.9 -6.3]	0.70	9.3 [5 – 22.2]
Urinary CN1 detection n(%)	22(48)	39(95)	<0.0001	3(33)	15(88)	0.007	18(72)
Homozygous(CTG) ₅ n(%)*	15 (37)	11 (28)	0.48	3 (43)	3 (18)	0.31	7(28)

Based on the observations that urinary CN1 concentrations were increased in macroalbuminuric patients regardless of the baseline disease (T2DM or CKD) and that urinary CN1 positively correlates with ACR, we assessed whether serum CN1 concentrations were decreased in these patients. To test this, all patients (n=111) were stratified on the basis of ACR in micro- (ACR \leq 300 mg/mg (n=53)) and macroalbuminuria (ACR>300 mg/mg (n=58)).

Although no differences in serum CN1 concentrations were found between micro and macroalbuminuric patients (**Fig. 8 A**), significantly lower serum CN1 levels were observed in all patients (n=111) when compared to the healthy subjects (4.1 μ g/ml [IQR 2.1-10.5 μ g/ml versus 9.3 μ g/ml [IQR 5.0 -22.2 μ g/ml], $p=0.0012$) (**Fig. 8 B**). These differences were not attributed to differences in genotype distribution (the (CTG)₅ homozygous vs. all other genotypes) as this was similar in both groups (healthy controls(72%) vs all patients (69%)($p> 0.05$)) (**Fig. 8 C**), but might rely on the higher proportion of females included in the healthy group (**Fig. 8 D**).

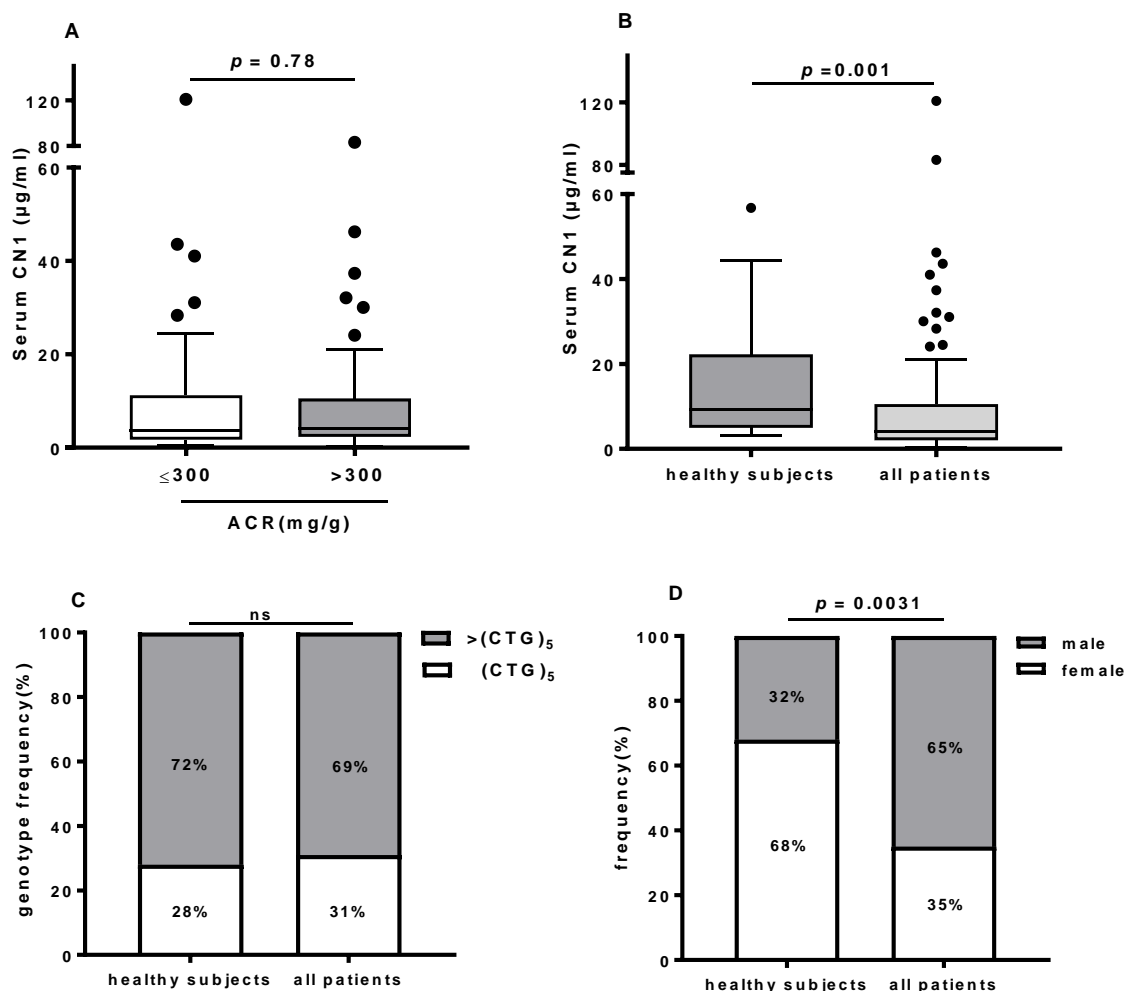


Fig.8 (A) Distribution of serum CN1 concentrations in the studied patients (n=111) according to ACR in: microalbuminuria (ACR \leq 300 mg/g) (n=53) and macroalbuminuria (ACR $>$ 300 mg/g) (n=56). Boxes and whiskers represent the median and IQR. **(B)** The patient's cohort display lower serum CN1 concentrations in comparison to healthy subjects. **(C)** Differences are not related to the distribution of the homozygous CNDP1 (CTG)₅ versus all other genotypes $>$ (CTG)₅ (p=ns). **(D)** The frequency of female distribution is higher in the healthy group (68%) in comparison to the patient's cohort (35%) (p=0.0031)

Interestingly, a modest but significant positive correlation between serum CN1 and urinary CN1 concentrations was observed for the whole cohort of patients (n=111) ($r=0.22$, $p=0.018$) **(Fig. 9 A)**.

Since the (CTG)_n polymorphism within the CNDP1 gene is known to influence CN1 concentrations in serum, we investigated whether this was also true for urinary CN1 concentrations. To test this, serum and urinary CN1 concentrations from healthy subjects and T2DM were stratified for genotype into (CTG)₅ homozygous versus other genotypes ($>$ (CTG)₅). Whereas healthy subjects homozygous for (CTG)₅ showed significant lower serum CN1 concentrations compared to healthy subjects carrying other CNDP1 genotypes (5.5 μ g/ml [IQR 3.2 – 9.1] versus 11.5 μ g/ml [IQR 5.5-31.1]; $p=0.017$), no differences in urinary CN1 concentrations in (CTG)₅ vs $>$ (CTG)₅ were found (81.3 ng/ml [IQR 0 - 146] vs 76.6 ng/ml [IQR 0 - 115.2]; $p=0.83$) **(Fig. 9 B)**. In T2DM patients, a trend towards lower median serum and urinary CN1 concentrations in the (CTG)₅ homozygous group compared to $>$ (CTG)₅ was observed but did not reach statistical significance (in serum: 3.5 μ g/ml [IQR 1.9 - 10.9] versus 4.4 μ g/ml [IQR 2.6 - 12.7], $p=0.62$ and in urine: 59.6 ng/ml [IQR 0- 503.2] vs 141.3 ng/ml [IQR 26.1- 718.5]; $p=0.14$ respectively) **(Fig. 9 C)**.

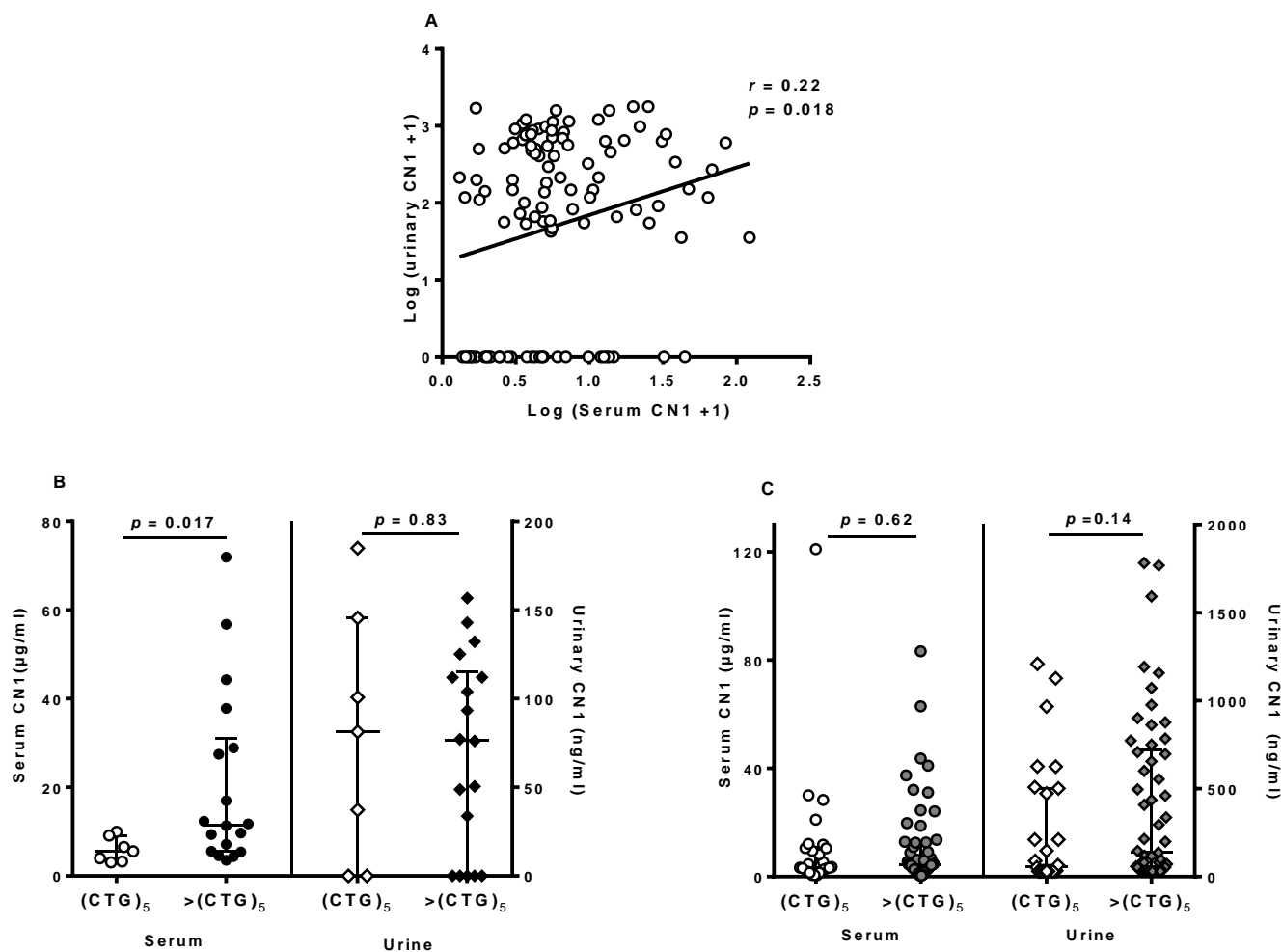


Fig.9 (A) Pearson correlation of serum CN1 (Log (Serum CN1 +1)) and urinary CN1 (Log (urinary CN1+1)) concentrations in all patients (n=111). **(B and C)** Distribution of serum CN1 (left y axis) and urinary CN1 concentrations (right y axis) according to CNDP1 genotype ((CTG)₅ homozygous versus other CNDP1 genotypes >(CTG)₅) in healthy subjects **(B)** and in patients with T2DM **(C)**. Results are expressed for each individual patient. The lines represents the median and IQR.

To gain more insight into the factors influencing urinary CN1 concentrations in the overall patient cohort (n=111), relevant kidney disease-associated variables i.e. age, sex, baseline kidney disease (T2DM or non-diabetic CKD), renal replacement therapy, serum CN1 concentrations, CNDP1(CTG)₅ homozygosity, eGFR and ACR were selected as independent predictors of log-transformed (urinary CN1 +1) (**Table 14.**). In univariate analysis, the variables sex, baseline disease and renal replacement therapy did not reach the significance threshold and were excluded in the subsequent multivariate model. The remaining variables with a p value <0.25 were included in the multivariate linear regression model (**Table 14.**). Multivariate

analysis revealed that albuminuria (ACR) and serum CN1 concentrations are the strongest predictors of urinary CN1 concentrations, all together explaining 44% of variation of urinary CN1 concentrations (log urinary CN1 +1) ($R^2 = 0.44$, $p < 0.0001$).

Table 14. Univariate and multivariate analysis of urinary CN1 in T2DM and CKD patients

Variable	Univariate analysis				Multivariate analysis			
	Coefficient (β)	95% CI		<i>p</i> -value	Coefficient (β)	95% CI		<i>p</i> -value
Age (years)	-0.012	-0.028	-0.003	0.11	0.003	-0.01	0.02	0.68
Female sex	-0.270	-0.76	0.22	0.27	-	-	-	-
non-diabetic kidney disease	0.150	-0.407	0.706	0.57	-	-	-	-
On renal replacement therapy	-0.195	-0.70	0.28	0.41	-	-	-	-
CNDP1 (CTG) ₅ homozygosity	-0.500	-0.9	0.001	0.050	-0.21	-0.61	0.18	0.29
Log (Serum CN1 +1)	0.605	0.093	1.118	0.021	0.65	0.25	0.04	0.002
Log (ACR)	0.630	0.48	0.79	<0.0001	0.89	0.65	1.13	<0.001
eGFR(ml/min/1.73 m ²)	-0.009	-0.017	-0.0003	0.042	0.001	-0.01	0.01	0.88

Univariate and multivariate regression models with log transformed (urinary CN1 +1) as the dependent variable. Goodness of fit of the multivariate regression full model: $R^2 = 0.44$; $p < 0.0001$

3.4 Toxicity profile of Methylglyoxal in human vascular endothelium

Methylglyoxal (MGO) is a reactive carbonyl species (RCS) mainly derived from glucose metabolism. Diabetes is associated with increased levels of RCS, which are believed to be implicated in the development of micro and macrovascular complications in these patients. In this section we investigated the susceptibility of human umbilical vein endothelial cells to MGO. To this end, HUVECs were treated with a wide range of MGO concentrations (100, 200, 400 and 800 μ M) over a period of 24 hours. Changes in cell morphology and impairment of cell viability were assessed by microscopy and MTT assay respectively. As depicted in **Fig.10 A**, cell detachment was already evident at 400 μ M of MGO and became worse at and 800 μ M. These changes were associated with a significant decrease of cell viability as assessed by MTT (**Fig. 10 B**). Toxicity towards 800 μ M of MGO was clearly dependent on the number of seeded cells, with lower numbers of seeded cells being more susceptible to MGO (**Fig. 10 C**).

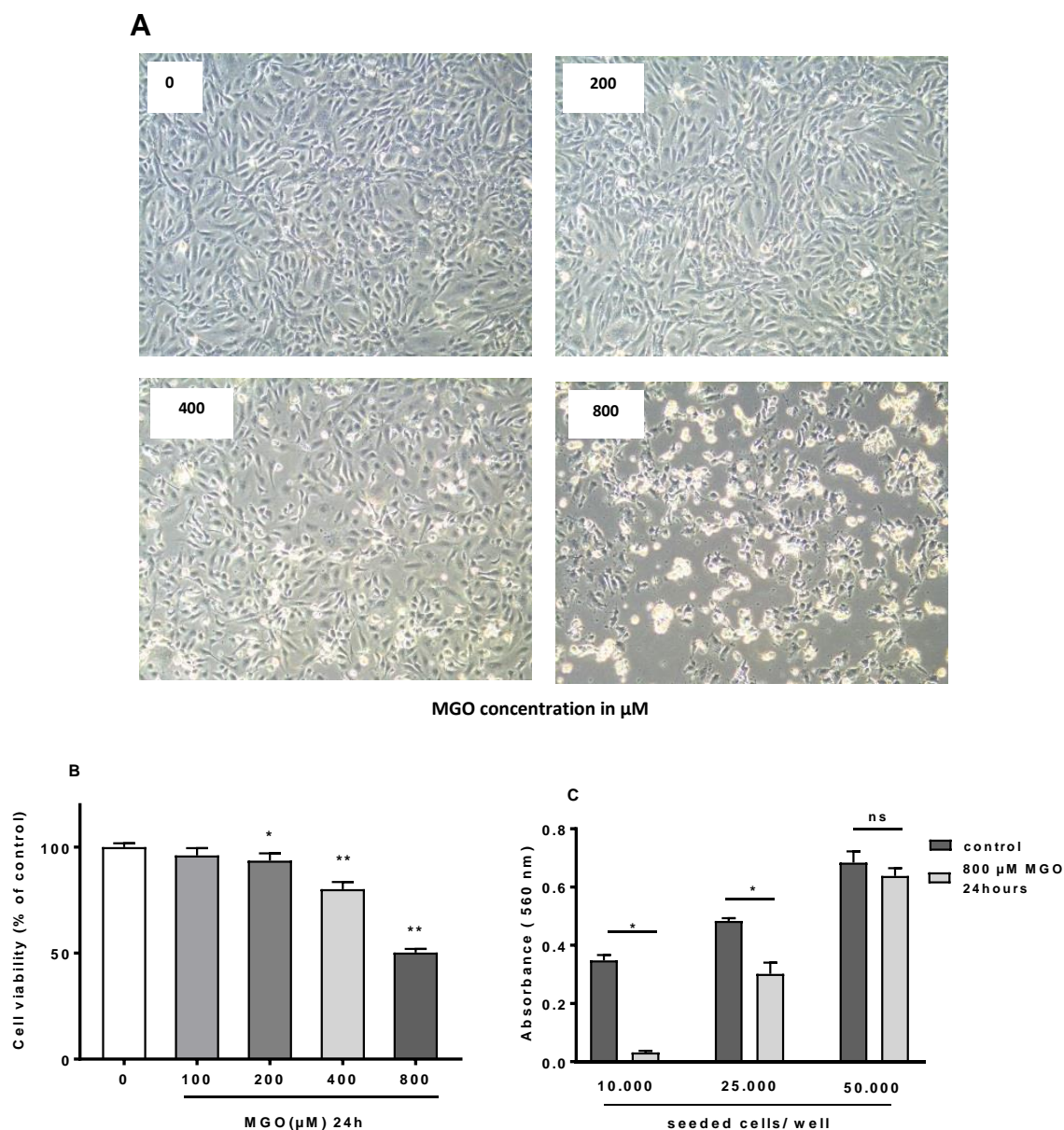


Fig. 10. Cytotoxicity of methylglyoxal after 24 hours. HUVECs were treated with different concentrations of MGO for 24 hours. Changes in cell morphology and cell viability were assessed by phase-contrast microscopy and MTT assay respectively. **(A)** Representative pictures of HUVECs treated with different concentrations of MGO. Original magnification 10x **(B)** Cells were seeded at a density of 25.000 cell/well and viability was measured by MTT and expressed as % of control cells not treated with MGO. Cell viability strongly decreased at 400μM and 800μM MGO ** $p < 0.0001$ compared to control (0 μM MGO). For each condition 6 replicates were used. **(C)** Toxicity towards 800 μM of MGO was tested against different densities of seeded cells (10.000, 25.000 and 50.000 cells/well). Note that at the highest cell density (50.000 cells/well) cell viability is no longer affected by 800 μM MGO.

To investigate if MGO-mediated toxicity was associated with DNA damage and cell apoptosis, TUNEL assay was performed. As depicted in **Fig. 11**, at concentrations of 800 μ M MGO an evident increased number of TUNEL positive cells were observed.

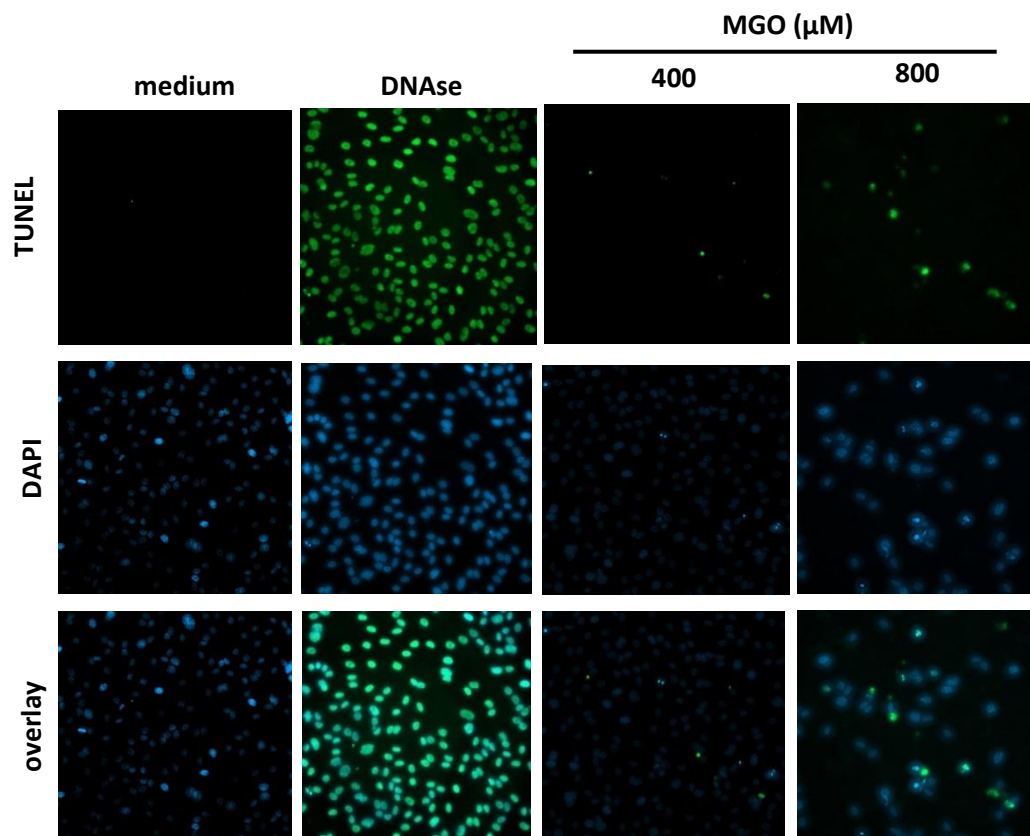


Fig. 11. MGO treatment induces apoptosis. HUVECs were treated for 24 hours with 400 or 800 μ M of MGO and detection of apoptotic cells was assessed by TUNEL assay. Medium: untreated cells, Dnase I treatment: Positive control. Magnification: 20x.

3.5 Carnosine treatment ameliorates MGO-induced toxicity

Based on the alleged anti-oxidative and RCS-chelating properties of carnosine we investigated whether MGO-induced toxicity can be mitigated by carnosine. This was studied in a chronic manner by exposing HUVECs for 7 days to MGO and more acutely in a type of “wound healing” setting, i.e. by assessing the ability of endothelial cells to repair a damage monolayer in the presence or absence of MGO.

Under MGO chronic exposure conditions, cell detachment was clearly visible already after 1 day of MGO treatment. Although at day 1 cell morphology was slightly

improved by 20 mM of L-carnosine, on subsequent days the endothelial cell monolayer greatly improved only when carnosine was present in the cell culture medium. This was substantiated by an increased number of cells attached to the culture plate which further proliferated, while in the absence of carnosine this was not observed **Fig.12**

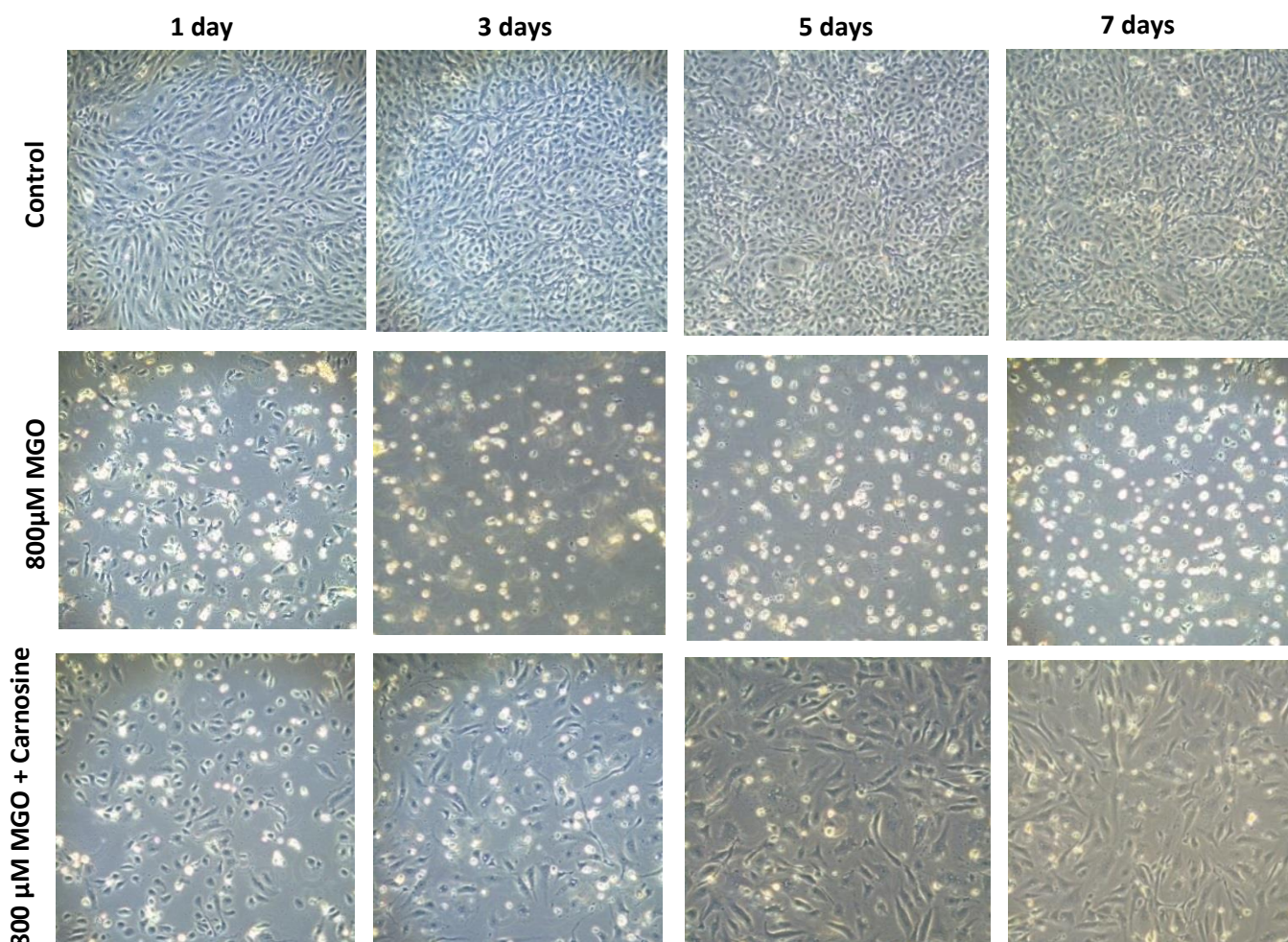


Fig.12. Carnosine prevents toxicity under MGO chronic challenge conditions. HUVECs were cultured for various time points in the presence of 800 μ M MGO (panel in the middle) or in the presence MGO and 20Mm Carnosine (lower panel). HUVECs cultured in normal medium (upper panel) served as control. Phase-contrast microscopy pictures were taken at 1, 3, 5 and at 7 days to assess morphological changes, magnification10x.

The results found in the chronic exposure experiments were in concordance to the results from the endothelial cell scratch assay. While in the control monolayers a complete recovery occurred within 24 hrs after initiation of the scratch, in the presence of MGO cells started to detach resulting in a complete disruption of the cell monolayer. At early time points (1 and 6 hrs) carnosine did not affect impairment of

the monolayer. However, at later time points (24 and 48 hrs) cell motility and proliferation appeared to recover, although to a lesser extent compared to untreated cells (**Fig. 13**).

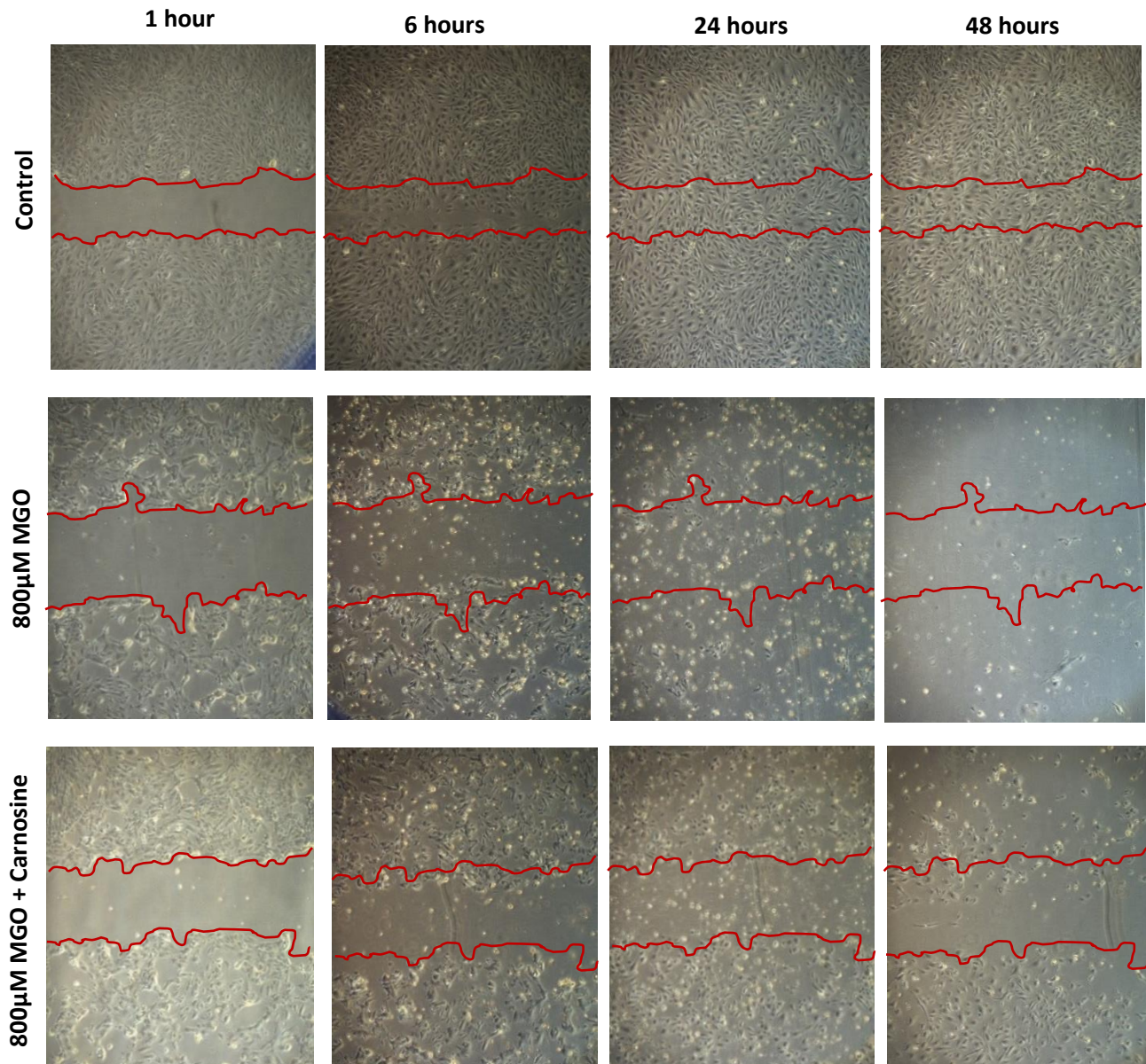


Fig. 13. Carnosine improves cell migration and proliferation in MGO treated cells.

Confluent HUVECs were challenged with 800µM MGO in the absence or presence of 20mM Carnosine (Car). A scratch with a p20 pipette tip was performed in the monolayer and the closure of the wound was imaged over 48 hours. Phase-contrast microscopy pictures of the wound area were taken at 1, 6, 24 and 48 hours after the scratch. The figure shows pictures of the extend of the closure obtained under control conditions (upper row), cells treated with 800 µM MGO (middle row) and cells treated with 800µM MGO and 20mM Carnosine (lower row). Red lines represent the border of the initial scratch. magnification10x.

3.6 Characterization of a green fluorescent protein (roGFP)-based redox biosensor

Changes in the reduction-oxidation (redox) state within cells and organisms are important reactions occurring in normal physiological processes like cell proliferation and growth but also in conditions where elevated and prolonged oxidative stress play a pivotal role, such as in diabetes and diabetes-related vascular complications.

In this paragraph we characterized a cytosolic green fluorescent protein (roGFP)-based redox sensor that allows the dynamic analysis of the redox state, with the intention to assess if MGO and or carnosine affect the intracellular redox milieu. This sensor is equipped with a redox-sensitive green fluorescent protein (GFP) that by the introduction of cysteine groups into the protein structure can modify its fluorescent properties. The fusion of the human enzyme glutaredoxin (Grx-1) which functions as glutathione-dependent oxidoreductase facilitates a specific, fast, dynamic and live visualization and measurement of the glutathione redox potential.

To explore the sensitivity of the roGFP redox sensor in living cells, we tested its response to exogenous added H_2O_2 and dithiothreitol (DTT), agents with well-known oxidizing and reducing properties, respectively. Addition of $50\mu\text{M}$ H_2O_2 in the medium of roGFP transduced HUVECs led to a strong and immediate oxidative response, evidenced by an increase in the excitation ratio (395/485 nm), and remained in the oxidative state until injection of $500\mu\text{M}$ DTT (**Fig.14 A**). These results indicate that roGFP is sensitive and respond within seconds to changes in the cell redox state. Of note, no changes in the redox potential were observed in non- transduced cells (data not shown).

To examine the sensitivity of roGFP to different concentrations of H_2O_2 , dose response experiments with concentrations within the μM range were performed. Injection of as little as $6\mu\text{M}$ H_2O_2 was sufficient to elicit a rapid increased of the excitation ratio. Consequently, injection of higher H_2O_2 concentrations i.e. $25\mu\text{M}$ and $50\mu\text{M}$ induced a higher increase in the excitation ratio which prolonged over 60 minutes (**Fig.14 B**).

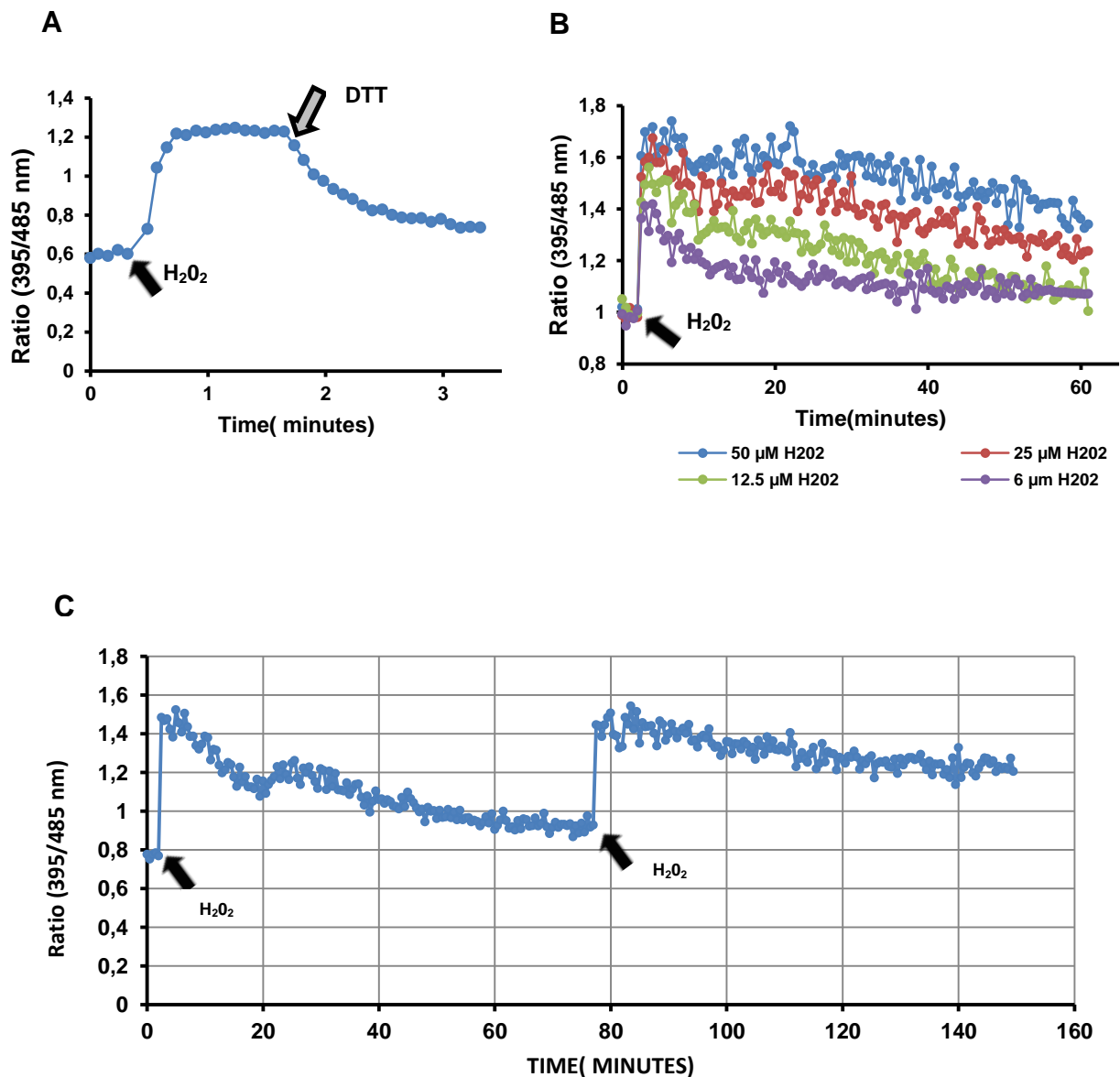


Fig.14 roGFP fusion protein allows dynamic visualization of rapid intracellular redox changes. HUVECs expressing roGFP were excited at 395 and 485 nm, and the ratio of emission at 528 was calculated and plotted against time (x axis). **(A)** Cells were treated with 50μM H₂O₂ followed by addition of 500μM DTT (dithiothreitol) 30 seconds later. **(B)** roGFP-expressing HUVECs were treated with the indicated concentrations of H₂O₂ at 1 minute and the radiometric sensor response was measured over time. **(C)** roGFP-expressing HUVECs were treated with one bolus of 50μM H₂O₂ at 2 minutes. Recovery of the cells from the oxidative state is evidenced by a gradual decline of the excitation ratio. After 77 minutes a second bolus of 50μM H₂O₂ was injected accompanied with a slower recovery from the oxidative state.

To examine the recovery of the HUVECs during repetitive oxidative injections, roGFP-expressing cells were consecutively challenged with H₂O₂. When cells were challenged for the first time with 50μM of H₂O₂ the excitation ratio rapidly increased followed by a gradual decline to near baseline in approximately 77 minutes. Also the

second H_2O_2 challenge resulted in a rapid increase of the excitation ratio, but the decline was much slower. Indeed, 77 minutes after the second injection the excitation ratio remained at the level of 1.20 pointing out that 94% of the roGFP-expressing cells were still in an oxidative state (**Fig.14 C**).

Since it has been suggested that endogenous oxidant levels are dependent on cell number, we tested whether the redox potential is influenced by cell density. roGFP-expressing HUVECs cells were seeded at different densities and the redox potential at baseline was determined. An association between cell density and redox state was observed. Accordingly, a higher cell density e.g. 40.000 cells/well led to a lower excitation ratio whereas a low cell density (10.000 cells/well) was associated with a higher ratio (**Fig.15 A**). To assess the response and recovery of different cells densities towards oxidative stress, we challenged cells seeded at different densities with $50\mu\text{M}$ H_2O_2 and the redox state was monitored over 50 minutes.

Interestingly, after an acute H_2O_2 injection, cells with the higher density showed a tendency towards a faster recovery reflected by a more rapid decline of the excitation ratio over time (**Fig.15 B**).

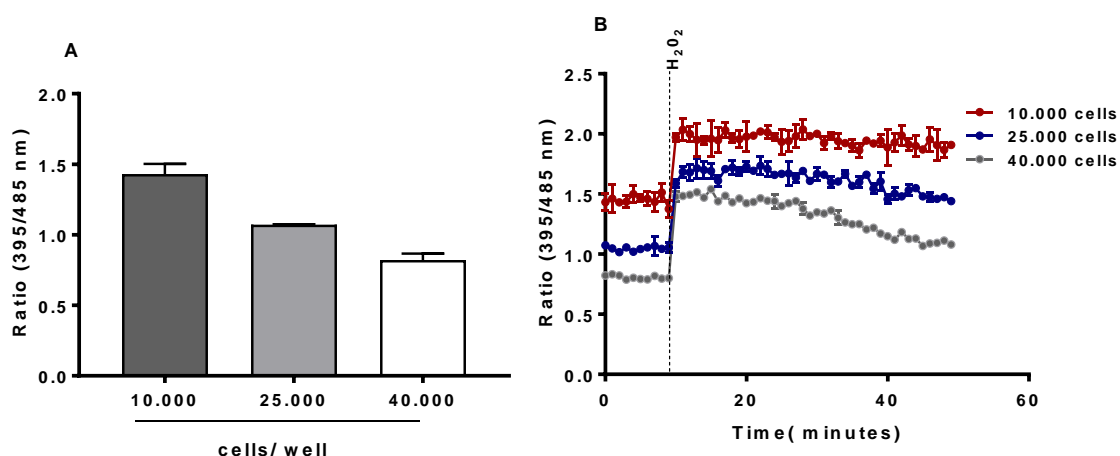


Fig.15. Cell density influences baseline redox state and recovery from oxidative stress. roGFP-expressing HUVECs were seeded at different densities (10.000, 25.000 and 40.000 cells/ 0.32 cm^2) and the excitation ratio at baseline was determined (**A**). After 5 minutes $50\mu\text{M}$ H_2O_2 was injected and the redox response was monitored over a 50-minute time frame. Error bars represent mean and SD.

Having assessed the characteristics of the roGFP-sensor we next studied the behavior of MGO and/or carnosine in this system.

Since morphological changes and decreased cell viability were previously observed with 200, 400 and 800 μ M MGO, roGFP expressing cells were challenged with similar concentrations. The redox response was monitored over a time frame of 30 minutes and compared to the redox changes elicited by a single bolus of 50 μ M H₂O₂.

A rapid increase from 1.0 to 1.7 in the excitation ratio was observed with 50 μ M H₂O₂ injection. In contrast, MGO elicited only a minimal increase in excitation ratio, by far less compared 50 μ M H₂O₂ (**Fig.16 A**). Since MGO-induced ROS production is likely to be time-dependent, cells were injected with 800 μ M MGO and the redox response was monitored over a longer period of time.

Directly before the challenge with MGO and at the end of the experiment changes in cell morphology were assessed by microscopy (**Fig.16 C**). While at 800 μ M MGO a clear cell morphological change was observed at the end of the response period, MGO elicited only a mild net increase of 0.2 in the excitation ratio which maintained during the time frame of 250 minutes without any further increase. Thus, compared to the oxidative response elicited by 50 μ M H₂O₂, changes in the excitation ratio by high concentrations of MGO are extremely low (**Fig.16 C**).

To test whether carnosine influences the intracellular redox milieu, roGFP-expressing HUVECs were first treated with 50 μ M of H₂O₂ and after 10 minutes, when the excitation ratio remained at a plateau, either with DTT or 20mM of carnosine were added. Both compounds were able to decrease the excitation ratio to a similar extent (**Fig. 16 B**).

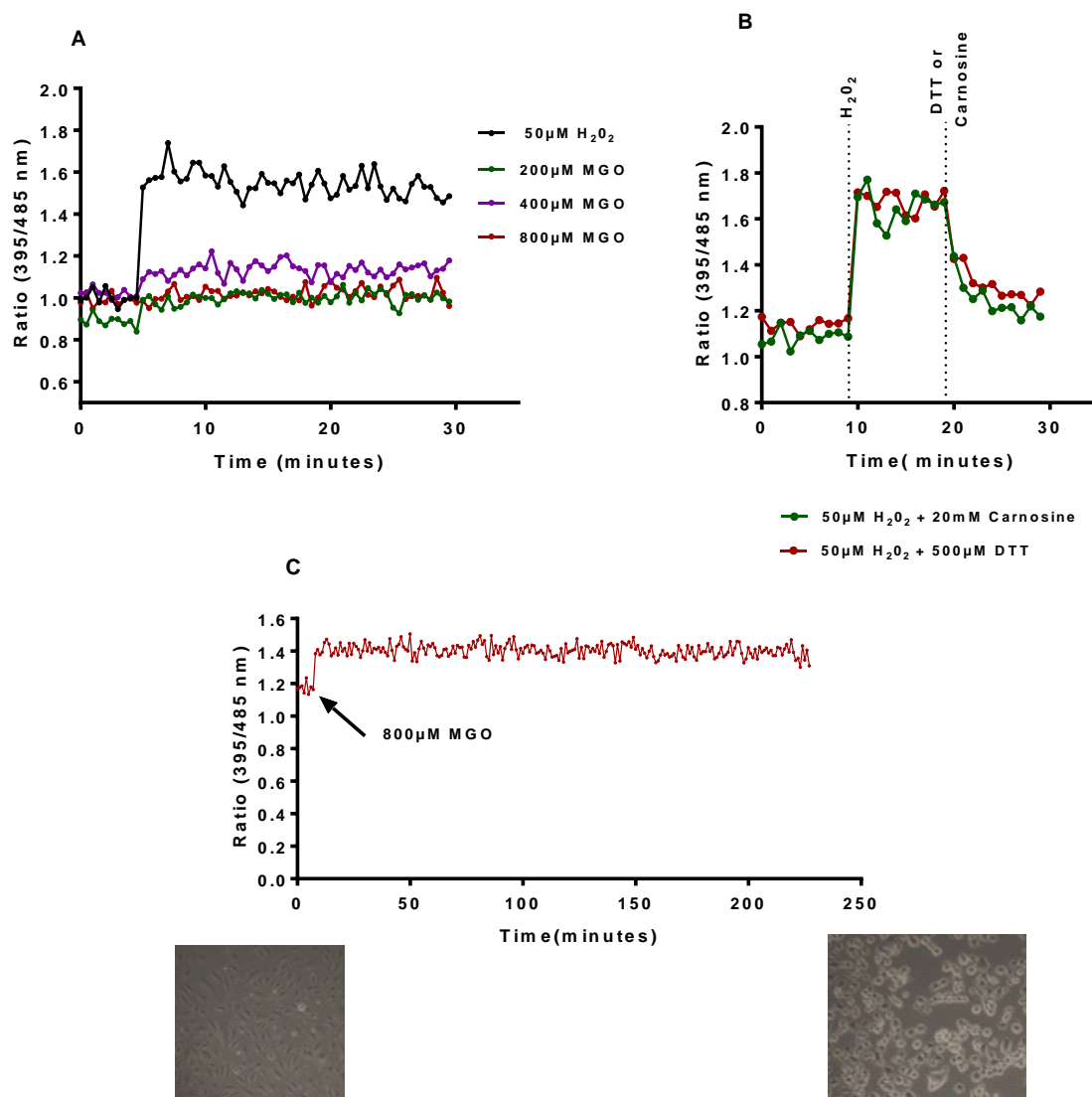


Fig.16 Redox response of roGFP- expressing cells to MGO and carnosine. (A) roGFP-expressing HUVECs were challenged at time = 5 minutes with different concentrations of MGO or 50 μM H_2O_2 . The redox response was monitored for a total time frame of 30 minutes. **(B)** HUVECs expressing roGFP were challenged with 50 μM H_2O_2 to elicit an increased excitation ratio. At time = 20 minutes either 20 mM of L-carnosine or 500 μM DTT was added. Note that the addition of either of these compounds elicited an immediate decrease in excitation ratio. **(C)** roGFP-expressing HUVECs were challenged with 800 μM of MGO and the redox response was monitored over 250 minutes. Simultaneously, morphologic changes induced by 800 μM MGO treatment were assessed by phase microscopy, magnification(10x)

4 DISCUSSION

4.1 Detection of Carnosinase1 in urine

Numerous studies have reported on CN1 in serum and cerebrospinal fluid (CSF). This is not surprising based on its tissue expression profile and the fact that CN1 is targeted to the secretory pathway⁷⁶. The results described herein indicate that besides serum and CSF, CN1 is also present in human urine.

The ELISA system employed herein has a high specificity as CN1 was undetectable in urine and serum of wild type mice, and measurable in serum (8.7- 30.4 $\mu\text{g/ml}$) and in urine (0 – 930.5 ng/ml) of transgenic animals overexpressing human CN1. However, it should be noted, that our ELISA system cannot differentiate between the different CN1 conformations i.e. monomers or homodimers.

Importantly, we were unable to detect any enzymatic activity of natural occurring CN1 in human or mouse urine. Yet, and as reported for other enzymes secreted in urine, lack of enzyme activity might be caused by several unfavorable factors intrinsic to urine i.e. high urea concentrations, longstanding retention in the bladder and low pH^{93,94}. Accordingly, the reported pH activity curve of CN1 shows a maximum between pH 7.5 - 8.5⁷⁶. Of note, the enzymatic activity of CN1 recombinant protein spiked in urine was measurable, although in a lesser extent compared to the recombinant CN1 spiked in assay buffer (5.7 $\mu\text{M/ml/h}$ vs 6.4 $\mu\text{M/ml/h}$). This strengthens the argument that urine may inhibit CN1 enzymatic activity. Based on these observations one would expect that longer incubations of the recombinant CN1 protein in urine might completely abolish enzymatic activity, however this was not assessed in the present study.

4.2 Characterization of 24-hr urinary CN1 in living kidney donors and patients with T2DM (DIALECT cohort)

To assess the relevance of urinary CN1 for renal function impairment in T2DM patients, CN1 was measured in 24-hr urine samples from patients with T2DM and living kidney donors (healthy subjects). Urinary CN1 was detected in 74% of the healthy subjects. In the group of diabetic patients, the proportion of urine samples in which CN1 was detected increased in parallel with the degree of albuminuria from

61% in the normoalbuminuric group, to 81% in the microalbuminuria group. In T2DM patients with macroalbuminuria, nearly all the urine samples (97%) were positive for CN1. In line with this, our results also show that high urinary CN1 excretion rates in T2DM patients correlates with increased albuminuria and low eGFR, which are the main prognostic predictors of diabetic nephropathy⁹⁵. Likewise, glycosuria appeared to be an independent factor influencing urinary CN1 concentrations.

An intrinsic carnosine metabolism in the human kidney has been reported based on the presence of carnosine synthesizing and degrading enzymes, i.e. carnosine synthase (CARNS) and CN1 respectively⁹⁰. Immune-histological studies in human kidneys, suggest that these enzymes are expressed in different compartments of the nephron. While carnosine synthesis in the proximal tubule might be important for protecting renal tissue from oxygen radicals, degradation of carnosine by CN1 in the distal tubule might play a role in maintaining a low pH, required for the exchange of H⁺ with K⁺ and Na⁺ ions in this compartment, as previously suggested by Peters et.al⁹⁰.

Glomerular filtration is restricted by the size and charge barrier of the glomerular basement membrane and the underlying slit diaphragm. It is believed that small negatively charged proteins such as albumin are not completely retained by the glomerular filtration barrier. Most of the filtrated albumin, does however not reach the lower urinary system as it is reabsorbed in the proximal tubule. In view of the molecular weight (~65kDa) and the isoelectric point of CN1 monomers, it is conceivable that monomeric CN1 may pass the filtration barrier with similar sieving characteristics as for albumin (~67kDa). In its homodimer conformation (~130kDa), which is believed to be the major conformation of CN1 in serum⁹⁶, CN1 is thus too large to cross the glomerular filtration barrier.

Small molecules like organic anions and cations (H⁺, creatinine, drug metabolites, etc.) are cleared from the blood via tubular secretion. This process requires specific transporters and mostly occurs in the proximal tubule and to a lesser extent in other segments of the nephron. Because tubular secretion is highly selective and CN1 transporters are not known to be present in the kidney, the presence of CN1 in urine cannot be explained by tubular secretion. Therefore, the appearance of CN1 in urine of healthy individuals might be due to 1) filtration of small amounts of CN1 monomers

from the circulation or 2) local renal production and secretion of CN1 into the tubular lumen.

In the T2DM group, CN1 was detected in nearly all patients. Among these patients, urinary CN1 excretion rates were significantly higher in patients with macroalbuminuria. Considering that the glomerular filtration barrier is severely impaired in such patients it is conceivable that, like albumin, CN1 will appear in the urine, which also explains the positive association between albuminuria and urinary CN1. Importantly, urinary CN1 excretion rates did not differ between healthy subjects and T2DM patients with microalbuminuria, presumably because the amount of filtered CN1 did not exceed the tubular reabsorption capacity in these patients. Thus, we speculate that similar as in healthy individuals, CN1 is predominately derived from local renal synthesis, or filtration of CN1 monomers in patients with microalbuminuria, rather than from glomerular filtration.

Typically, in the course of DN, an increase in albuminuria precedes the decline in glomerular filtration rate. The results herein show that T2DM patients with kidney disease, as reflected by poor eGFR, display high urinary CN1 excretion rates. Multivariate linear regression analysis suggests that both albuminuria and eGFR can be considered as independent factors associated with urinary CN1. Hence, our findings suggest that urinary CN1 excretion increases along with renal function deterioration, yet they also warrant further large prospective studies to confirm these cross-sectional findings. Likewise, glycosuria also appeared as an independent factor positively associated with urinary CN1. If CN1 is locally synthesized in the kidney, it is possible that high glucose levels in the tubular lumen enhance CN1 secretion, similar as described by Riedl et. al⁹⁷.

4.3 Association of serum CN1 and CNDP1 genotype with urinary CN1 in patients with T2DM and non-diabetic chronic kidney disease (Mannheim Cohort).

Proteinuria, routinely assessed in patients with chronic kidney disease (CKD), is a well-established biomarker for the progression of renal function deterioration⁹⁸. Assessment of proteinuria based on 24-hr urine collection has been considered as

the gold standard. Yet, because of its inconvenience and collection inaccuracies^{99,100} clinical practice guidelines suggest first void or spot urine albumin-to-creatinine ratio (ACR) as a surrogate of the albumin excretion rate¹⁰¹.

To test if our findings in 24-hr urine would be similar as in spot urine (Results, section 3.2) we performed a feasibility study in a smaller group of CKD patients to assess the relation between CN1 in spot urine, ACR and renal function. Additionally, the influence of serum CN1 concentrations and CNDP1 genotype on urinary CN1 expression was tested.

In agreement with the observations described in section 3.2 we found that urinary CN1 is more frequently detected and displays higher concentrations in patients with macroalbuminuria as compared to those with microalbuminuria.

In a similar fashion, a strong positive correlation between urinary CN1 and ACR was found ($r=0.66$, $p < 0.0001$). Furthermore, patients with strongly to moderately impaired renal function (eGFR < 60 ml/min) displayed higher urinary CN1 concentrations compared to patients with preserved renal function (147.5 vs 17 ng/ml, $p=0.015$).

In multivariate regression analysis, ACR and serum CN1 concentrations appeared as independent predictors of urinary CN1, explaining together 44 % of variation of urinary CN1 concentrations ($R^2 = 0.44$, $p < 0.0001$). These data are concordant to our previous results using 24-hr urine samples and thus suggest that spot urine can be used for the assessment of CN1 in biorepositories in which spot - rather than 24-hr urine samples were collected.

Based on the findings that urinary CN1 concentrations are increased in patients with macroalbuminuria, one would expect that as a result of an impaired glomerular barrier, serum CN1 concentrations would be decreased in this group. Contrary to our expectations, no differences in serum CN1 concentration were found between patients with micro and macroalbuminuria.

Nonetheless, lower serum CN1 concentrations were observed in all patients when compared to the healthy group. In this regard, one of the possible factors influencing serum CN1 concentrations is the high prevalence of protein energy wasting, defined as a “state of decreased body stores of protein and energy fuels”, among patients with CKD¹⁰². In support of this, low serum CN1 concentrations have also been reported in pathologies characterized by a high catabolic state, e.g. neoplasia and liver cirrhosis^{103–105}, making protein energy wasting, a likely factor influencing serum

CN1 concentrations in patients with residual renal function. Alternatively, dialysis per se and metabolic acidosis, a common comorbidity of CKD, can promote enhanced protein breakdown and amino acid oxidation^{106,107}.

Yet, the strong correlation between urinary CN1 concentrations and albuminuria suggests that increasing CN1 concentrations likely reflects impairment of the glomerular filtration barrier. This may also partly explain the positive correlation between serum CN1 and urinary CN1 concentrations in patients but not in healthy controls (data not shown), as in patients with an impaired glomerular filtration barrier such a correlation would be expected.

In the multivariate regression model serum CN1 was identified as independent predictor of urinary CN1 concentrations. Likewise, positive correlations between albumin synthesis and albumin urinary excretion have been reported in patients with macroalbuminuria¹⁰⁸.

Inasmuch as renal CN1 mRNA and protein expression have been reported^{77,79,90} to the best of our knowledge there are no studies that provide direct evidence for renal CN1 secretion into the renal tubular lumen. Yet, the lack of correlation between serum and urinary CN1 concentrations in healthy individuals argues against a free communication between the circulatory and urinary compartment and tempted us to presume that urinary CN1 in healthy conditions is a consequence of renal production and secretion. Nonetheless, it cannot be excluded that if serum CN1 partly exist in a monomeric conformation it might pass the filtration barrier¹⁰⁹.

In contrast to serum CN1 concentrations, it appeared that urinary CN1 concentrations were not influenced by the CNDP1 (CTG)_n polymorphism. Since it has been shown that variations in the leucine repeat in the signal peptide of CN1 affects CN1 secretion this would have also been expected for renal CN1 secretion⁸⁸. If, however monomeric serum CN1 is filtered, urinary CN1 concentrations will correlate more with the fraction of monomeric CN1 rather than the CNDP1 genotype. Of note, our in-house ELISA used for CN1 detection cannot distinguish between CN1 monomers and dimers and the small amount of CN1 as well as the presence of urea in the urine samples also hamper drawing firm conclusions in Westernblotting experiments.

Although patients with low eGFR appeared to have higher urinary CN1 concentrations compared to patients with preserved renal function (<60 ml/min) and

the univariate analysis revealed a significant negative correlation between eGFR and urinary CN1, the subsequent multivariate regression model excluded eGFR as an independent explanatory factor for urinary CN1. This could be explained by 1) the current study population in overall has considerable renal function impairment compared to the subjects studied in section 3.2 and thus it is conceivable that in late stages of disease, eGFR to a lesser extent influences urinary CN1 concentrations; 2) A possible collinearity between the variables eGFR and ACR may add similar information and thus only the variable with the strongest relationship is included in the final regression model¹¹⁰.

Multivariate linear regression analysis revealed that albuminuria (ACR) and serum CN1 can be considered as independent predictors of urinary CN1 in non-diabetic and diabetic patients with CKD. If we speculate that in this group of patients, the majority of detected CN1 in urine originates from the circulation, these findings might imply that concentrations of CN1 in urine is a function of two independent processes: on one hand the change in glomerular permselectivity reflected by a strong positive correlation with albuminuria and on the other hand the ability of the liver to maintain CN1 production.

Even though the findings herein are in concordance with the observations drawn from the 24-hr urine, there are some limitations. Firstly, the number of healthy controls is relatively small and healthy controls were not matched for gender and age with the patient's cohort. Hence, conclusions based on any direct comparisons between patients and controls cannot be firmly drawn and should be taken with caution. Secondly, it would be useful to directly compare 24-hr urine and spot urine of the same individual. We are aware that this would have been the most ideal situation, however, at the time of study 24-hr urine samples were not available for most of the patients. The intention of this study was to assess the feasibility of meaningful measuring urinary CN1 concentrations in spot urine.

4.4 Toxicity profile of Methylglyoxal in human vascular endothelium

Compelling evidence suggest that glycation may play a role in the pathophysiology of microvascular complications. MGO, the prototypical RCS, has been found to accumulate in tissues under diabetic conditions. We studied the susceptibility of cultured human vascular endothelial cells towards MGO.

MGO dose-dependently decreased the viability of HUVECs when challenged for 24 hrs. This was most pronounced for concentrations of 400 and 800 μ M of MGO. Our findings are in concordance with previous reports where cytotoxicity was seen in a similar concentration ranges¹¹¹. MGO also increased the number of TUNEL positive cells, yet the percentage hereof was low (approximately 10%) and thus DNA damage alone cannot explain MGO's toxicity.

It should be emphasized that the concentrations used herein and in other studies appeared to be higher than levels reported *in vivo* in T2DM patients, albeit that the circulating MGO concentrations reported in humans largely differ between different studies.

Our results also demonstrated that higher cell densities markedly reduced the sensitivity of endothelial cells to MGO. The mechanism by which higher cell densities decrease susceptibility was not address in this study, but presumably this effect underlies a simple decrease in the number of MGO molecules available per cell with increasing cell density.. In line with this, different susceptibilities of low and high cell densities to other compounds i.e. cadmium and zinc oxide effects have also been described^{112,113}.

Although in this study we did not address the mechanism by which MGO exert cytotoxicity, it has been reported that MGO can induce apoptosis by caspase activation, suppression of the anti-apoptotic proteins Bcl-2 and XIAP(X-linked inhibitor of pro-apoptosis protein) and by upregulation of proapoptotic signals such as Bax^{111,114}. Considering this, one would expect that at high MGO concentrations, the majority of cells, if not all, would be TUNEL positive. Hence our data suggest that other cell death mechanisms, such as necrosis may occur upon a challenge with high MGO concentrations. In line with this assumption, a recent study in epithelial cells demonstrated that MGO treatment indeed triggers both necrosis and apoptosis¹¹⁵.

4.5 Carnosine treatment ameliorates MGO-induced toxicity

Carnosine has been repeatedly described as a RCS scavenger, by forming stable adducts through covalent bonds with RCS¹¹⁶. *In vivo* studies have shown that carnosine supplementation in Zucker rats and BTBR^{ob/ob} mice results in an increased amount of carnosine-HNE-MA, carnosine-DHN and 3-HPMA adducts in urine along

with a decrease of urinary markers of protein carbonylation^{65,117}. The authors suggest that this might be a means to detoxify and remove RCS from the body. Our own data are to some extent in line with this assumption, as it demonstrates the beneficial effect of carnosine on MGO-mediated toxicity, suggesting a potential role in detoxification by carnosine. Nonetheless, it should be underscored that the quenching activity of carnosine is strong towards α and β unsaturated carbonyls, but rather poor for dicarbonyls such as MGO¹¹⁶. A more recent study revealed that carnosine catalyzes the formation of transient MGO oligomers rather than forming a stable covalent bond¹¹⁸. Hence, carnosine's protective effects reported herein are unlikely due to its scavenging ability, but rather to other mechanisms involved in the carnosine-MGO interaction. Since MGO also induces oxidative stress in endothelial cells, we postulated that carnosine's protective effects might be explained by its antioxidative properties. Alternatively, carnosine might also act extracellularly preventing cellular uptake of MGO, as proposed by others¹¹⁸. A recent study in human endothelial cells, demonstrated that carnosine can reverse MGO-induced effects on expression of cell cycle-associated genes.⁵¹ Of note, the protective effect of carnosine on cell viability was not assessed by MTT assay, but was based on the morphological changes observed upon co-treatment with carnosine.

4.6 Characterization of a green fluorescent protein (roGFP)-based redox biosensor

Fluorescent based redox probes have important advantages such as high specificity and easy subcellular targeting. The sensor described herein is based on the ability of RoGFP to become oxidized or reduced in response of changes in the cytosolic redox couple GSH/GSSG acting as a Grx-1 target protein⁵⁷. The roGFP sensor described in the experimental part of this thesis was constructed by substitution of specific surface-exposed residues with cysteines that have not been reported elsewhere. It has two fluorescence excitation maxima at 395 and 485 and an emission peak at 528nm. In principal, any compound that interacts with the equilibrium between GSH/GSSG can be screened with this biosensor.

Our results confirmed the observations of Gutscher et. al, suggesting that the fusion of Grx-1 facilitates a rapid visualization of glutathione redox changes⁵⁷. Furthermore, the sensor responds to concentrations as low as 6 μ M of exogenously added oxidizing agents such as H₂O₂. The effect of cell density on the redox status previously reported was also observed in our hands⁵⁷.

It has been reported that MGO promotes oxidative stress by inducing the production of ROS which in turn might change the redox potential¹¹⁹. Based on this, we investigated whether MGO-induced ROS can be detected by roGFP-expressing HUVECs. Against our expectations, we did not observe changes in the redox status upon short (30 mins) and long treatment with MGO (250 mins) (Fig.16. A,C). As such, attempts to detect MGO-induced ROS were not successful, even though it is reported that MGO detoxification through the glyoxalase (GLO) pathway is glutathione (GSH)-dependent. Masterjohn et al. described that acute glutathione depletion induces MGO accumulation by impairing its detoxification¹²⁰.

Our findings were unexpected since MGO clearly inflicts morphological changes after short times of incubation (Fig. 13). Additionally, it is reported that MGO-induced H₂O₂ generation is detected at 15 min (47.5%) and increases to 96.7% at 1 hour in comparison to untreated cells¹¹⁵. In a previous version of roGFP, Dooley et.al were also unable to demonstrate any response to stimuli reported to generate intracellular H₂O₂⁵⁴.

MGO is mainly detoxified by the glyoxalase system and its cofactor, GSH, it is not depleted but recycled back into the system¹²¹. Hence, there is no net change in GSH concentrations, which might explain why our roGFP sensor does not show fluctuations in the redox status upon an MGO challenge. Importantly, and similar to DTT, our results also showed that carnosine decreases the excitation ratio after H₂O₂ injection, thus confirming its anti-oxidative properties.

5 CONCLUSION

Our studies demonstrate for the first time that CN1 can be detected in spot and 24-hr urine of healthy individuals, patients with T2DM and non-diabetic CKD. These findings are compatible with previous immune-histological and mRNA data that showed that CN1 is expressed in human renal tissue⁹⁰. The physiological role of urinary CN1 is, however, still elusive and warrants further studies to assess its relevance for renal carnosine stores. Furthermore, our results suggest that the in-house ELISA system can be employed to measure CN1 in different matrixes i.e. serum and urine, from both human and mouse.

Urinary CN1 concentrations appeared to be increased in patients with macroalbuminuria regardless of the baseline disease, and to be associated with renal function. Noteworthy, the correlation coefficient between urinary CN1 and albuminuria (ACR) in spot urine (section 3.3) was higher and the model goodness of fit was even better than the one reported in the 24-hr urine study (section 3.2)

($r = 0.59$ vs 0.66) and ($R^2 = 0.37$, $p < 0.0001$ vs 0.44 , $p < 0.0001$). The strong correlations found and the confirmatory nature of the data indeed suggest that urinary CN1 can be reliably measured in spot urine and warrants further studies in large cohorts to assess the potential relevance hereof for renal function deterioration. The confirmation and reproducibility of the findings from the 24-hr urine study in the present data suggest that the assessment of CN1 in spot samples can be considered as reliable as in 24-hr samples.

Our in vitro studies suggest that MGO affects cell viability in a dose dependent manner. Based on the low cell number positive for TUNEL, we assume that MGO-induced cell death is not completely mediated through apoptosis. Carnosine appeared to counteract MGO-induced toxicity in vitro. Since there is no reported evidence for scavenging of MGO by carnosine, the beneficial effects of carnosine might be due to its antioxidant properties rather than through a scavenging mechanism

6 REFERENCES

1. International Diabetes Federation, IDF diabetes Atlas - 2017 8th edn. Brussels, Belgium: International Diabetes Federation, 2017 [Internet]. 2017 Available from: <https://diabetesatlas.org/>
2. Forouhi NG, Wareham NJ: Epidemiology of diabetes. *Medicine (Abingdon)*. 42: 698–702, 2014
3. Morris AP, Voight BF: Large-scale association analysis provides insights into the genetic architecture and pathophysiology of type 2 diabetes. *Nat. Genet.* 44: 981–990, 2012
4. Morgan CL, Currie CJ, Peters JR: Relationship between diabetes and mortality: a population study using record linkage. *Diabetes Care* 23: 1103–7, 2000
5. Wei M, Gaskill SP, Haffner SM, Stern MP: Effects of diabetes and level of glycemia on all-cause and cardiovascular mortality. The San Antonio Heart Study. *Diabetes Care* 21: 1167–72, 1998
6. Stratton IM, Adler AI, Neil HA, Matthews DR, Manley SE, Cull CA, Hadden D, Turner RC, Holman RR: Association of glycaemia with macrovascular and microvascular complications of type 2 diabetes (UKPDS 35): prospective observational study. *BMJ* 321: 405–412, 2000
7. Matheus AS de M, Tannus LRM, Cobas RA, Palma CCS, Negrato CA, Gomes M de B: Impact of Diabetes on Cardiovascular Disease: An Update. *Int. J. Hypertens.* 2013: 1–15, 2013
8. Morrish NJ, Wang SL, Stevens LK, Fuller JH, Keen H: Mortality and causes of death in the WHO Multinational Study of Vascular Disease in Diabetes. *Diabetologia* 44 Suppl 2: S14-21, 2001
9. American Association Diabetes. Classification and Diagnosis of Diabetes: Standards of Medical Care in Diabetes—2018. *Diabetes Care* 41: S13–S27, 2018
10. Committee IE: International Expert Committee Report on the Role of the A1C Assay in the Diagnosis of Diabetes. *Diabetes Care* 32: 1327, 2009
11. American Diabetes Association AD: Diagnosis and classification of diabetes mellitus. *Diabetes Care* 34 Suppl 1: S62-9, 2011
12. UKPDS Group: Tight blood pressure control and risk of macrovascular and microvascular complications in type 2 diabetes: UKPDS 38. UK Prospective Diabetes Study Group. *BMJ* 317: 703–13, 1998
13. Beckman JA, Creager MA, Libby P: Diabetes and atherosclerosis: epidemiology, pathophysiology, and management. *JAMA* 287: 2570–81, 2002
14. Buse JB, Ginsberg HN, Bakris GL, Clark NG, Costa F, Eckel R, Fonseca V, Gerstein HC, Grundy S, Nesto RW, Pignone MP, Plutzky J, Porte D, Redberg R, Stitzel KF, Stone NJ: Primary Prevention of Cardiovascular Diseases in People With Diabetes Mellitus: A scientific statement from the American Heart Association and the American Diabetes Association. *Diabetes Care* 30: 162–172, 2007
15. Colhoun HM, Betteridge DJ, Durrington PN, Hitman GA, Neil HA, Livingstone SJ, Thomason MJ, Mackness MI, Charlton-Menys V, Fuller JH, CARDS investigators: Primary prevention of cardiovascular disease with atorvastatin in type 2 diabetes in the Collaborative Atorvastatin Diabetes Study

- (CARDS): multicentre randomised placebo-controlled trial. *Lancet* 364: 685–696, 2004
16. King P, Peacock I, Donnelly R: The UK Prospective Diabetes Study (UKPDS): clinical and therapeutic implications for type 2 diabetes. *Br. J. Clin. Pharmacol.* 48: 643–648, 2001
 17. Duckworth WC, McCarren M, Abraira C, VA Diabetes Trial: Glucose control and cardiovascular complications: the VA Diabetes Trial. *Diabetes Care* 24: 942–5, 2001
 18. Nathan DM, Cleary PA, Backlund J-YC, Genuth SM, Lachin JM, Orchard TJ, Raskin P, Zinman B, Diabetes Control and Complications Trial/Epidemiology of Diabetes Interventions and Complications (DCCT/EDIC) Study Research Group: Intensive diabetes treatment and cardiovascular disease in patients with type 1 diabetes. *N. Engl. J. Med.* 353: 2643–53, 2005
 19. Group TAC: Intensive Blood Glucose Control and Vascular Outcomes in Patients with Type 2 Diabetes. *N. Engl. J. Med.* 358: 2560–2572, 2008
 20. Marso SP, Daniels GH, Brown-Frandsen K, Kristensen P, Mann JFE, Nauck MA, Nissen SE, Pocock S, Poulter NR, Ravn LS, Steinberg WM, Stockner M, Zinman B, Bergenstal RM, Buse JB, LEADER Steering Committee, LEADER Trial Investigators: Liraglutide and Cardiovascular Outcomes in Type 2 Diabetes. *N. Engl. J. Med.* 375: 311–322, 2016
 21. Marso SP, Bain SC, Consoli A, Eliaschewitz FG, Jódar E, Leiter LA, Lingvay I, Rosenstock J, Seufert J, Warren ML, Woo V, Hansen O, Holst AG, Pettersson J, Vilsbøll T: Semaglutide and Cardiovascular Outcomes in Patients with Type 2 Diabetes. *N. Engl. J. Med.* 375: 1834–1844, 2016
 22. Neal B, Perkovic V, Mahaffey KW, de Zeeuw D, Fulcher G, Erondu N, Shaw W, Law G, Desai M, Matthews DR: Canagliflozin and Cardiovascular and Renal Events in Type 2 Diabetes. *N. Engl. J. Med.* 377: 644–657, 2017
 23. Yehya A, Sadhu AR: New Therapeutic Strategies for Type 2 Diabetes CME. *Methodist Debaquey Cardiovasc. J.* 14: 281–288, 2018
 24. Roberts S, Barry E, Craig D, Airoidi M, Bevan G, Greenhalgh T: Preventing type 2 diabetes: systematic review of studies of cost-effectiveness of lifestyle programmes and metformin, with and without screening, for pre-diabetes. *BMJ Open* 7: e017184, 2017
 25. Reutens AT, Atkins RC: Epidemiology of diabetic nephropathy. *Contrib. Nephrol.* 170: 1–7, 2011
 26. National Institutes of Health, National Institute of Diabetes and Digestive and Kidney Diseases, Bethesda, MD 2017.: United States Renal Data System. 2017USRDS annual data report: Epidemiology of kidney disease in the United States [Internet]. Available from: www.usrds.org
 27. Lopes AA: End-stage renal disease due to diabetes in racial/ethnic minorities and disadvantaged populations. *Ethn. Dis.* 19: S1-47–51, 2009
 28. Cusick M, Meleth AD, Agrón E, Fisher MR, Reed GF, Knatterud GL, Barton FB, Davis MD, Ferris FL, Chew EY, Early Treatment Diabetic Retinopathy Study Research Group: Associations of mortality and diabetes complications in patients with type 1 and type 2 diabetes: early treatment diabetic retinopathy study report no. 27. *Diabetes Care* 28: 617–25, 2005
 29. Adler AI, Stevens RJ, Manley SE, Bilous RW, Cull CA, Holman RR, UKPDS Group: Development and progression of nephropathy in type 2 diabetes: The United Kingdom Prospective Diabetes Study (UKPDS 64). *Kidney Int.* 63: 225–232, 2003
 30. Tonneijck L, Muskiet MHA, Smits MM, van Bommel EJ, Heerspink HJL, van

- Raalte DH, Joles JA: Glomerular Hyperfiltration in Diabetes: Mechanisms, Clinical Significance, and Treatment. *J. Am. Soc. Nephrol.* 28: 1023–1039, 2017
31. KDIGO: Chapter 1: Definition and classification of CKD. *Kidney Int. Suppl.* 3: 19–62, 2013
 32. Pugliese G: Updating the natural history of diabetic nephropathy. *Acta Diabetol.* 51: 905–915, 2014
 33. Mogensen CE: Microalbuminuria, blood pressure and diabetic renal disease: Origin and development of ideas. *Diabetologia.* 42: 263–285, 1999
 34. Ponchiardi C, Mauer M, Najafian B: Temporal Profile of Diabetic Nephropathy Pathologic Changes. *Curr. Diab. Rep.* 13: 592–599, 2013
 35. Amin AP, Whaley-Connell AT, Li S, Chen S-C, McCullough PA, Kosiborod MN, KEEP Investigators: The Synergistic Relationship Between Estimated GFR and Microalbuminuria in Predicting Long-term Progression to ESRD or Death in Patients With Diabetes: Results From the Kidney Early Evaluation Program (KEEP). *Am. J. Kidney Dis.* 61: S12–S23, 2013
 36. Umanath K, Lewis JB: Update on Diabetic Nephropathy: Core Curriculum 2018. *Am. J. Kidney Dis.* 71: 884–895, 2018
 37. Lewis EJ, Hunsicker LG, Clarke WR, Berl T, Pohl MA, Lewis JB, Ritz E, Atkins RC, Rohde R, Raz I, Collaborative Study Group: Renoprotective Effect of the Angiotensin-Receptor Antagonist Irbesartan in Patients with Nephropathy Due to Type 2 Diabetes. *N. Engl. J. Med.* 345: 851–860, 2001
 38. Brenner BM, Cooper ME, de Zeeuw D, Keane WF, Mitch WE, Parving H-H, Remuzzi G, Snapinn SM, Zhang Z, Shahinfar S, RENAAL Study Investigators: Effects of Losartan on Renal and Cardiovascular Outcomes in Patients with Type 2 Diabetes and Nephropathy. *N. Engl. J. Med.* 345: 861–869, 2001
 39. Haller H, Ito S, Izzo JL, Januszewicz A, Katayama S, Menne J, Mimran A, Rabelink TJ, Ritz E, Ruilope LM, Rump LC, Viberti G, ROADMAP Trial Investigators: Olmesartan for the Delay or Prevention of Microalbuminuria in Type 2 Diabetes. *N. Engl. J. Med.* 364: 907–917, 2011
 40. Ismail-Beigi F, Craven T, Banerji MA, Basile J, Calles J, Cohen RM, Cuddihy R, Cushman WC, Genuth S, Grimm RH, Hamilton BP, Hoogwerf B, Karl D, Katz L, Krikorian A, O'Connor P, Pop-Busui R, Schubart U, Simmons D, Taylor H, Thomas A, Weiss D, Hramiak I: Effect of intensive treatment of hyperglycaemia on microvascular outcomes in type 2 diabetes: an analysis of the ACCORD randomised trial. *Lancet* 376: 419–430, 2010
 41. Moraru A, Wiederstein J, Pfaff D, Fleming T, Miller AK, Nawroth P, Telesman AA: Elevated Levels of the Reactive Metabolite Methylglyoxal Recapitulate Progression of Type 2 Diabetes. *Cell Metab.* 27: 926–934.e8, 2018
 42. Kalapos MP: Where does plasma methylglyoxal originate from? *Diabetes Res. Clin. Pract.* 99: 260–271, 2013
 43. Miyata T, Horie K, Ueda Y, Fujita Y, Izuhara Y, Hirano H, Uchida K, Saito A, Van Ypersele De Strihou C, Kurokawa K: Advanced glycation and lipidoxidation of the peritoneal membrane: Respective roles of serum and peritoneal fluid reactive carbonyl compounds. *Kidney Int.* 58: 425–435, 2000
 44. Semchyshyn HM: Reactive carbonyl species in vivo: generation and dual biological effects. *ScientificWorldJournal.* 2014: 417842, 2014
 45. Guo Q, Mori T, Jiang Y, Hu C, Osaki Y, Yoneki Y, Sun Y, Hosoya T, Kawamata A, Ogawa S, Nakayama M, Miyata T, Ito S: Methylglyoxal contributes to the development of insulin resistance and salt sensitivity in Sprague–Dawley rats. *J. Hypertens.* 27: 1664–1671, 2009

46. Nigro C, Raciti GA, Leone A, Fleming TH, Longo M, Prevezano I, Fiory F, Mirra P, D'Esposito V, Ulianich L, Nawroth PP, Formisano P, Beguinot F, Miele C: Methylglyoxal impairs endothelial insulin sensitivity both in vitro and in vivo. *Diabetologia* 57: 1485–1494, 2014
47. Riboulet-Chavey A, Pierron A, Durand I, Murdaca J, Giudicelli J, Van Obberghen E: Methylglyoxal impairs the insulin signaling pathways independently of the formation of intracellular reactive oxygen species. *Diabetes* 55: 1289–99, 2006
48. Giacco F, Du X, D'Agati VD, Milne R, Sui G, Geoffrion M, Brownlee M: Knockdown of glyoxalase 1 mimics diabetic nephropathy in nondiabetic mice. *Diabetes* 63: 291–9, 2014
49. Miyazawa N, Abe M, Souma T, Tanemoto M, Abe T, Nakayama M, Ito S: Methylglyoxal augments intracellular oxidative stress in human aortic endothelial cells. *Free Radic. Res.* 44: 101–107, 2010
50. Yamawaki H, Saito K, Okada M, Hara Y: Methylglyoxal mediates vascular inflammation via JNK and p38 in human endothelial cells. *Am. J. Physiol. Physiol.* 295: C1510–C1517, 2008
51. Braun JD, Pastene DO, Breedijk A, Rodriguez A, Hofmann BB, Sticht C, von Ochsenstein E, Allgayer H, van den Born J, Bakker S, Hauske SJ, Krämer BK, Yard BA, Albrecht T: Methylglyoxal down-regulates the expression of cell cycle associated genes and activates the p53 pathway in human umbilical vein endothelial cells. *Sci. Rep.* 9: 1152, 2019
52. Thornalley PJ: The glyoxalase system: new developments towards functional characterization of a metabolic pathway fundamental to biological life. *Biochem. J.* 269: 1–11, 1990
53. Hanson GT, Aggeler R, Oglesbee D, Cannon M, Capaldi RA, Tsien RY, Remington SJ: Investigating Mitochondrial Redox Potential with Redox-sensitive Green Fluorescent Protein Indicators. *J. Biol. Chem.* 279: 13044–13053, 2004
54. Dooley CT, Dore TM, Hanson GT, Jackson WC, Remington SJ, Tsien RY: Imaging Dynamic Redox Changes in Mammalian Cells with Green Fluorescent Protein Indicators. *J. Biol. Chem.* 279: 22284–22293, 2004
55. Meyer AJ, Dick TP: Fluorescent Protein-Based Redox Probes. *Antioxid. Redox Signal.* 13: 621–650, 2010
56. Lukyanov KA, Belousov V V.: Genetically encoded fluorescent redox sensors. *Biochim. Biophys. Acta - Gen. Subj.* 1840: 745–756, 2014
57. Gutscher M, Pauleau A-L, Marty L, Brach T, Wabnitz GH, Samstag Y, Meyer AJ, Dick TP: Real-time imaging of the intracellular glutathione redox potential. *Nat. Methods* 5: 553–559, 2008
58. Bhaskar A, Chawla M, Mehta M, Parikh P, Chandra P, Bhave D, Kumar D, Carroll KS, Singh A: Reengineering Redox Sensitive GFP to Measure Mycothiol Redox Potential of Mycobacterium tuberculosis during Infection. *PLoS Pathog.* 10: e1003902, 2014
59. Drozak J, Veiga-da-Cunha M, Vertommen D, Stroobant V, Van Schaffingen E: Molecular Identification of Carnosine Synthase as ATP-grasp Domain-containing Protein 1 (ATPGD1). *J. Biol. Chem.* 285: 9346–9356, 2010
60. Mannion AF, Jakeman PM, Dunnett M, Harris RC, Willan PL: Carnosine and anserine concentrations in the quadriceps femoris muscle of healthy humans. *Eur. J. Appl. Physiol. Occup. Physiol.* 64: 47–50, 1992
61. Boldyrev AA, Aldini G, Derave W: Physiology and Pathophysiology of Carnosine. *Physiol. Rev.* 93: 1803–1845, 2013

62. Baguet A, Koppo K, Pottier A, Derave W: β -Alanine supplementation reduces acidosis but not oxygen uptake response during high-intensity cycling exercise. *Eur. J. Appl. Physiol.* 108: 495–503, 2010
63. Soliman KM, Mohamed AM, Metwally NS: Attenuation of some metabolic deteriorations induced by diabetes mellitus using carnosine. *J. Appl. Sci.* 7: 2252–2260, 2007
64. Sauerhöfer S, Yuan G, Braun GS, Deinzer M, Neumaier M, Gretz N, Floege J, Kriz W, van der Woude F, Moeller MJ: L-carnosine, a substrate of carnosinase-1, influences glucose metabolism. *Diabetes* 56: 2425–32, 2007
65. Albrecht T, Schilperoort M, Zhang S, Braun JD, Qiu J, Rodriguez A, Pastene DO, Krämer BK, Köppel H, Baelde H, de Heer E, Anna Altomare A, Regazzoni L, Denisi A, Aldini G, van den Born J, Yard BA, Hauske SJ: Carnosine Attenuates the Development of both Type 2 Diabetes and Diabetic Nephropathy in BTBR ob/ob Mice. *Sci. Rep.* 7: 44492, 2017
66. Riedl E, Pfister F, Braunagel M, Brinkkötter P, Sternik P, Deinzer M, Bakker SJL, Henning RH, van den Born J, Krämer BK, Navis G, Hammes H-P, Yard B, Koepfel H: Carnosine Prevents Apoptosis of Glomerular Cells and Podocyte Loss in STZ Diabetic Rats. *Cell. Physiol. Biochem.* 28: 279–288, 2011
67. Ansurudeen I, Sunkari VG, Grünler J, Peters V, Schmitt CP, Catrina S-B, Brismar K, Forsberg EA: Carnosine enhances diabetic wound healing in the db/db mouse model of type 2 diabetes. *Amino Acids* 43: 127–134, 2012
68. Aydın AF, Küçükgergin C, Özdemirler-Erata G, Koçak-Toker N, Uysal M: The effect of carnosine treatment on prooxidant–antioxidant balance in liver, heart and brain tissues of male aged rats. *Biogerontology* 11: 103–109, 2010
69. Szwergold BS: Carnosine and anserine act as effective transglycating agents in decomposition of aldose-derived Schiff bases. *Biochem. Biophys. Res. Commun.* 336: 36–41, 2005
70. Seidler NW, Yeargans GS, Morgan TG: Carnosine disaggregates glycated α -crystallin: an in vitro study. *Arch. Biochem. Biophys.* 427: 110–115, 2004
71. Alhamdani M-SS, Al-Kassir A-HA-M, Abbas FKH, Jaleel NA, Al-Taee MF: Antiglycation and Antioxidant Effect of Carnosine against Glucose Degradation Products in Peritoneal Mesothelial Cells. *Nephron Clin. Pract.* 107: c26–c34, 2007
72. Aldini G, Carini M, Beretta G, Bradamante S, Facino RM: Carnosine is a quencher of 4-hydroxy-nonenal: through what mechanism of reaction? *Biochem. Biophys. Res. Commun.* 298: 699–706, 2002
73. Aldini G, Facino RM, Beretta G, Carini M: Carnosine and related dipeptides as quenchers of reactive carbonyl species: from structural studies to therapeutic perspectives. *Biofactors* 24: 77–87, 2005
74. de Courten B, Jakubova M, de Courten MP, Kukurova IJ, Vallova S, Krumpolec P, Valkovic L, Kurdiová T, Garzon D, Barbaresi S, Teede HJ, Derave W, Krssak M, Aldini G, Ukropec J, Ukropcova B: Effects of carnosine supplementation on glucose metabolism: Pilot clinical trial. *Obesity (Silver Spring)*. 24: 1027–34, 2016
75. Regazzoni L, de Courten B, Garzon D, Altomare A, Marinello C, Jakubova M, Vallova S, Krumpolec P, Carini M, Ukropec J, Ukropcova B, Aldini G: A carnosine intervention study in overweight human volunteers: bioavailability and reactive carbonyl species sequestering effect. *Sci. Rep.* 6: 27224, 2016
76. Teufel M, Saudek V, Ledig J-P, Bernhardt A, Boularand S, Carreau A, Cairns NJ, Carter C, Cowley DJ, Duverger D, Ganzhorn AJ, Guenet C, Heintzelmann B, Laucher V, Sauvage C, Smirnova T: Sequence identification and

- characterization of human carnosinase and a closely related non-specific dipeptidase. *J. Biol. Chem.* 278: 6521–31, 2003
77. Janssen B, Hohenadel D, Brinkkoetter P, Peters V, Rind N, Fischer C, Rychlik I, Cerna M, Romzova M, de Heer E, Baelde H, Bakker SJL, Zirie M, Rondeau E, Mathieson P, Saleem MA, Meyer J, Köppel H, Sauerhoefer S, Bartram CR, Nawroth P, Hammes H-P, Yard BA, Zschocke J, van der Woude FJ: Carnosine as a protective factor in diabetic nephropathy: association with a leucine repeat of the carnosinase gene CNDP1. *Diabetes* 54: 2320–7, 2005
 78. Freedman BI, Hicks PJ, Sale MM, Pierson ED, Langefeld CD, Rich SS, Xu J, McDonough C, Janssen B, Yard BA, van der Woude FJ, Bowden DW: A leucine repeat in the carnosinase gene CNDP1 is associated with diabetic end-stage renal disease in European Americans. *Nephrol. Dial. Transplant.* 22: 1131–1135, 2007
 79. Mooyaart AL, van Valkengoed IGM, Shaw PKC, Peters V, Baelde HJ, Rabelink TJ, Bruijn JA, Stronks K, de Heer E: Lower frequency of the 5/5 homozygous CNDP1 genotype in South Asian Surinamese. *Diabetes Res. Clin. Pract.* 85: 272–278, 2009
 80. Mooyaart AL, Zutinic A, Bakker SJL, Grootendorst DC, Kleefstra N, van Valkengoed IGM, Bohringer S, Bilo HJG, Dekker FW, Bruijn JA, Navis G, Janssen B, Baelde HJ, De Heer E: Association Between CNDP1 Genotype and Diabetic Nephropathy Is Sex Specific. *Diabetes* 59: 1555–1559, 2010
 81. Kim S, Abboud HE, Pahl M V., Tayek J, Snyder S, Tamkin J, Alcorn H, Ipp E, Nast CC, Elston RC, Iyengar SK, Adler SG: Examination of Association with Candidate Genes for Diabetic Nephropathy in a Mexican American Population. *Clin. J. Am. Soc. Nephrol.* 5: 1072–1078, 2010
 82. Mcdonough CW, Hicks PJ, Lu L, Langefeld CD, Freedman BI, Bowden DW: The Influence of Carnosinase Gene Polymorphisms on Diabetic Nephropathy Risk in African Americans NIH Public Access. *Hum Genet* 126: 265–275, 2009
 83. Craig DW, Millis MP, DiStefano JK: Genome-wide SNP genotyping study using pooled DNA to identify candidate markers mediating susceptibility to end-stage renal disease attributed to Type 1 diabetes. *Diabet. Med.* 26: 1090–1098, 2009
 84. Wanic K, Placha G, Dunn J, Smiles A, Warram JH, Krolewski AS: Exclusion of Polymorphisms in Carnosinase Genes (CNDP1 and CNDP2) as a Cause of Diabetic Nephropathy in Type 1 Diabetes: Results of Large Case-Control and Follow-Up Studies. *Diabetes* 57: 2547, 2008
 85. Alkhalaf A, Bakker SJL, Bilo HJG, Gans ROB, Navis GJ, Postmus D, Forsblom C, Groop PH, Vionnet N, Hadjadj S, Marre M, Parving HH, Rossing P, Tarnow L: A polymorphism in the gene encoding carnosinase (CNDP1) as a predictor of mortality and progression from nephropathy to end-stage renal disease in type 1 diabetes mellitus. *Diabetologia* 53: 2562–8, 2010
 86. Peters V, Kebbewar M, Janssen B, Hoffmann GF, Möller K, Wygoda S, Charbit M, Fernandes-Teixeira A, Jeck N, Zschocke J, Schmitt CP, Schäfer F, Wühl E, for the ESCAPE Trial Group: CNDP1 genotype and renal survival in pediatric nephropathies. *J. Pediatr. Endocrinol. Metab.* 29: 827–33, 2016
 87. Kiliś-Pstrusińska K, Zwolińska D, Grzeszczak W, Study Group: Is carnosinase 1 gene (CNDP1) polymorphism associated with chronic kidney disease progression in children and young adults? results of a family-based study. *Arch. Med. Res.* 41: 356–62, 2010
 88. Riedl E, Koeppel H, Brinkkoetter P, Sternik P, Steinbeisser H, Sauerhoefer S, Janssen B, van der Woude FJ, Yard BA: A CTG polymorphism in the CNDP1 gene determines the secretion of serum carnosinase in Cos-7 transfected cells.

- Diabetes* 56: 2410–3, 2007
89. Zhang S, Albrecht T, Rodriguez-Niño A, Qiu J, Schnuelle P, Peters V, Schmitt CP, van den Born J, Bakker SJL, Lammert A, Krämer BK, Yard BA, Hauske SJ: Carnosinase concentration, activity, and CNDP1 genotype in patients with type 2 diabetes with and without nephropathy. *Amino Acids* 51: 611–617, 2019
 90. Peters V, Klessens CQF, Baelde HJ, Singler B, Veraar KAM, Zutinic A, Drozak J, Zschocke J, Schmitt CP, de Heer E: Intrinsic carnosine metabolism in the human kidney. *Amino Acids* 47: 2541–50, 2015
 91. Gant CM, Binnenmars SH, Berg E van den, Bakker SJL, Navis G, Laverman GD: Integrated Assessment of Pharmacological and Nutritional Cardiovascular Risk Management: Blood Pressure Control in the DIABetes and LifEstyle Cohort Twente (DIALECT). *Nutrients* 9: 709, 2017
 92. Adelman K, Frey D, Riedl E, Koepfel H, Pfister F, Peters V, Schmitt CP, Sternik P, Hofmann S, Zentgraf HW, Navis G, van den Born J, Bakker SJL, Krämer BK, Yard BA, Hauske SJ: Different conformational forms of serum carnosinase detected by a newly developed sandwich ELISA for the measurements of carnosinase concentrations. *Amino Acids* 43: 143–151, 2012
 93. Jung K, Pergande M, Schreiber G, Schröder K: Stability of enzymes in urine at 37 degrees C. *Clin. Chim. Acta.* 131: 185–91, 1983
 94. Jung K, Pergande M, Schröder K, Schreiber G: Influence of pH on the activity of enzymes in urine at 37 degrees C. *Clin. Chem.* 28: 1814, 1982
 95. Berhane AM, Weil EJ, Knowler WC, Nelson RG, Hanson RL: Albuminuria and estimated glomerular filtration rate as predictors of diabetic end-stage renal disease and death. *Clin. J. Am. Soc. Nephrol.* 6: 2444–51, 2011
 96. Pavlin M, Rossetti G, De Vivo M, Carloni P: Carnosine and Homocarnosine Degradation Mechanisms by the Human Carnosinase Enzyme CN1: Insights from Multiscale Simulations. *Biochemistry* 55: 2772–84, 2016
 97. Riedl E, Koepfel H, Pfister F, Peters V, Sauerhoefer S, Sternik P, Brinkkoetter P, Zentgraf H, Navis G, Henning RH, Van Den Born J, Bakker SJL, Janssen B, van der Woude FJ, Yard BA: N -Glycosylation of Carnosinase Influences Protein Secretion and Enzyme Activity. *Diabetes* 59: 1984–1990, 2010
 98. Gansevoort RT, Matsushita K, van der Velde M, Astor BC, Woodward M, Levey AS, de Jong PE, Coresh J, Chronic Kidney Disease Prognosis Consortium: Lower estimated GFR and higher albuminuria are associated with adverse kidney outcomes. A collaborative meta-analysis of general and high-risk population cohorts. *Kidney Int.* 80: 93–104, 2011
 99. Côté A-M, Firoz T, Mattman A, Lam EM, von Dadelszen P, Magee LA: The 24-hour urine collection: gold standard or historical practice? *Am. J. Obstet. Gynecol.* 199: 625.e1-6, 2008
 100. Rodby RA: Timed Urine Collections for Albumin and Protein: “The King Is Dead, Long Live the King!” *Am. J. Kidney Dis.* 68: 836–838, 2016
 101. Johnson DW, Atai E, Chan M, Phoon RK, Scott C, Toussaint ND, Turner GL, Usherwood T, Wiggins KJ: KHA-CARI Guideline: Early chronic kidney disease: Detection, prevention and management. *Nephrology* 18: 340–350, 2013
 102. Jadeja YP, Kher V: Protein energy wasting in chronic kidney disease: An update with focus on nutritional interventions to improve outcomes. *Indian J. Endocrinol. Metab.* 16: 246–51, 2012
 103. Arner P, Henjes F, Schwenk JM, Darmanis S, Dahlman I, Iresjö B-M, Naredi P, Agustsson T, Lundholm K, Nilsson P, Rydén M: Circulating carnosine dipeptidase 1 associates with weight loss and poor prognosis in gastrointestinal cancer. *PLoS One* 10: e0123566, 2015

104. Gautam P, Nair SC, Gupta MK, Sharma R, Polisetty RV, Uppin MS, Sundaram C, Puligopu AK, Ankathi P, Purohit AK, Chandak GR, Harsha HC, Sirdeshmukh R: Proteins with altered levels in plasma from glioblastoma patients as revealed by iTRAQ-based quantitative proteomic analysis. *PLoS One* 7: e46153, 2012
105. Peters V, Jansen EEW, Jakobs C, Riedl E, Janssen B, Yard BA, Wedel J, Hoffmann GF, Zschocke J, Gotthardt D, Fischer C, Köppel H: Anserine inhibits carnosine degradation but in human serum carnosinase (CN1) is not correlated with histidine dipeptide concentration. *Clin. Chim. Acta.* 412: 263–7, 2011
106. Greiber S, Mitch WE: Mechanisms for protein catabolism in uremia: metabolic acidosis and activation of proteolytic pathways. *Miner. Electrolyte Metab.* 18: 233–6, 1992
107. Lim VS, Kopple JD: Protein metabolism in patients with chronic renal failure: role of uremia and dialysis. *Kidney Int.* 58: 1–10, 2000
108. Kaysen GA, Gambertoglio J, Felts J, Hutchison FN: Albumin synthesis, albuminuria and hyperlipemia in nephrotic patients. *Kidney Int.* 31: 1368–76, 1987
109. Peters V, Kebbewar M, Jansen EW, Jakobs C, Riedl E, Koeppl H, Frey D, Adelman K, Klingbeil K, Mack M, Hoffmann GF, Janssen B, Zschocke J, Yard BA: Relevance of allosteric conformations and homocarnosine concentration on carnosinase activity. *Amino Acids* 38: 1607–15, 2010
110. Lang T: Documenting Research in Scientific Articles: Guidelines for Authors. *Chest* 131: 628–632, 2007
111. Yuan J, Zhu C, Hong Y, Sun Z, Fang X, Wu B, Li S: The role of cPLA2 in Methylglyoxal-induced cell apoptosis of HUVECs. *Toxicol. Appl. Pharmacol.* 323: 44–52, 2017
112. Banfalvi G, Ujvarosi K, Trencsenyi G, Somogyi C, Nagy G, Basnakian A: Cell culture density dependent toxicity and chromatin changes upon cadmium treatment in murine pre-B-cells. *Apoptosis* 12: 1219–1228, 2007
113. Papavlassopoulos H, Mishra YK, Kaps S, Paulowicz I, Abdelaziz R, Elbahri M, Maser E, Adelung R, Röhl C: Toxicity of Functional Nano-Micro Zinc Oxide Tetrapods: Impact of Cell Culture Conditions, Cellular Age and Material Properties. *PLoS One* 9: e84983, 2014
114. Jang JH, Kim E-A, Park H-J, Sung E-G, Song I-H, Kim J-Y, Woo C-H, Doh K-O, Kim KH, Lee T-J: Methylglyoxal-induced apoptosis is dependent on the suppression of c-FLIPL expression via down-regulation of p65 in endothelial cells. *J. Cell. Mol. Med.* 21: 2720–2731, 2017
115. Chan C-M, Huang D-Y, Huang Y-P, Hsu S-H, Kang L-Y, Shen C-M, Lin W-W: Methylglyoxal induces cell death through endoplasmic reticulum stress-associated ROS production and mitochondrial dysfunction. *J. Cell. Mol. Med.* 20: 1749–60, 2016
116. Vistoli G, Colzani M, Mazzolari A, Gilardoni E, Rivaletto C, Carini M, Aldini G: Quenching activity of carnosine derivatives towards reactive carbonyl species: Focus on α -(methylglyoxal) and β -(malondialdehyde) dicarbonyls. *Biochem. Biophys. Res. Commun.* 492: 487–492, 2017
117. Orioli M, Aldini G, Benfatto MC, Maffei Facino R, Carini M: HNE Michael Adducts to Histidine and Histidine-Containing Peptides as Biomarkers of Lipid-Derived Carbonyl Stress in Urines: LC-MS/MS Profiling in Zucker Obese Rats. *Anal. Chem.* 79: 9174–9184, 2007
118. Weigand T, Singler B, Fleming T, Nawroth P, Klika KD, Thiel C, Baelde H, Garbade SF, Wagner AH, Hecker M, Yard BA, Amberger A, Zschocke J,

- Schmitt CP, Peters V: Carnosine Catalyzes the Formation of the Oligo/Polymeric Products of Methylglyoxal. *Cell. Physiol. Biochem.* 46: 713–726, 2018
119. Liu C, Huang Y, Zhang Y, Chen X, Kong X, Dong Y: Intracellular methylglyoxal induces oxidative damage to pancreatic beta cell line INS-1 cell through Ire1 α -JNK and mitochondrial apoptotic pathway. *Free Radic. Res.* 51: 337–350, 2017
120. Masterjohn C, Mah E, Park Y, Pei R, Lee J, Manautou JE, Bruno RS: Acute glutathione depletion induces hepatic methylglyoxal accumulation by impairing its detoxification to d -lactate. *Exp. Biol. Med.* 238: 360–369, 2013
121. Morgenstern J, Fleming T, Schumacher D, Eckstein V, Freichel M, Herzig S, Nawroth P: Loss of Glyoxalase 1 Induces Compensatory Mechanism to Achieve Dicarbonyl Detoxification in Mammalian Schwann Cells. *J. Biol. Chem.* 292: 3224–3238, 2017

7 CURRICULUM VITAE

PERSONAL

Family name and first name: Rodríguez Niño, Maria Angelica

Date of birth: 13.11.1988

Place of birth: Bogota, Colombia

Marital status: Single

Father: Rodríguez Fernando

Mother: Niño Claudia

SCHOOL EDUCATION

02. 1995 – 12.2005 Middle school - Colegio Calasanz Femenino

UNIVERSITY EDUCATION

01.2006 – 12.2011 Bachelor of Human Medicine
Fundacion Universitaria de Ciencias de la Salud

09.2013 – 08.2015 Master of Science
University of Groningen

01.2016 – 03.2019 MD student GRK 1874/2
University of Heidelberg

04.2019– now PhD student
University of Groningen

8 ACKNOWLEDGMENTS

I would like to sincerely thank my supervisor Prof. Benito Yard, who gave me the opportunity to join his working group. I highly appreciate the patience, optimism and kindness you showed throughout our many discussions.

I would like to give my acknowledgements to Prof. Hans-Peter Hammes and the Graduate School DIAMICOM (GRK1874/2) who not only financed my project, but also support my scientific development.

I am also deeply grateful for the help and kindness of my dear coworkers: Sara Medina, Diego Pastene and Katharina Kohl. Thanks for not only sharing an office with me, but also your help, thoughts and resilience during the long days in the lab.

I would like to sincerely thank Jiedong Qiu, Rahef Ouerdani, Dan Feng, Shiqi Zang, Xia Li, Lisa Leikeim, Thomas Albrecht, Jana Braun and Prama Pallavi for your scientific input and support.

I owe my thanks to all the colleagues in the lab: Mrs. Annette Breedjik, Mrs. Renate Stein, Mrs. Katharina Prem and Mrs. Silke Deiter who taught me the experimental techniques and who were also patient and warm-hearted.